Algal Research 94 (2026) 104566

Contents lists available at ScienceDirect

Algal Research

journal homepage: www.elsevier.com/locate/algal

HPCCC-guided biorefinery strategy for the scalable recovery and biofunctional evaluation of diadinoxanthin from the diatom *Phaeodactylum tricornutum*

Daniela Bárcenas-Pérez [a,b], Maria Rita Garcia [c], Nelson G.M. Gomes [c], Paula B. Andrade [c], Arantzazu Sierra-Ramirez [d], Jakub Zápal [e], Marek Kuzma [e,f], Gergely Ernő Lakatos [a], Martin Lukeš [a], Pavel Hrouzek [a], Pablo J. Fernandez-Marcos [d], José Cheel [a,*]

[a] *Laboratory of Algal Biotechnology – Centre ALGATECH, Institute of Microbiology of the Czech Academy of Sciences, Opatovický mlýn, 379 81, Třeboň, Czech Republic*
[b] *Faculty of Science, University of South Bohemia, Branišovská 1760, 370 05, České Budějovice, Czech Republic*
[c] *REQUIMTE/LAQV, Laboratório de Farmacognosia, Departamento de Química, Faculdade de Farmácia, Universidade do Porto, 4050-313, Porto, Portugal*
[d] *Metabolic Syndrome Group—BIOPROMET, Madrid Institute for Advanced Studies—IMDEA Food,CEI UAM+CSIC, 28049, Madrid, Spain*
[e] *Laboratory of Molecular Structure Characterization, Institute of Microbiology of the Czech Academy of Sciences, Vídeňská 1083, 142 20, Prague, Czech Republic*
[f] *Department of Analytical Chemistry, Faculty of Science, Palacký University, 17. listopadu 12, 771 46, Olomouc, Czech Republic*

ARTICLE INFO

Keywords:
Diadinoxanthin
Diatoms
Countercurrent chromatography (CCC)
High performance countercurrent chromatography (HPCCC)
Centrifugal partition chromatography (CPC)

ABSTRACT

A high performance countercurrent chromatography (HPCCC)-guided biorefinery strategy was developed for the scalable recovery and biofunctional assessment of diadinoxanthin from the diatom *Phaeodactylum tricornutum*. A biphasic solvent system of *n*-heptane, ethyl acetate, ethanol, and water (5:4:5:3, *v/v/v/v*) was identified as optimal for both extraction and HPCCC separation. The process was successfully scaled from a 24 mL to a 134 mL HPCCC column using volumetric scale-up principles, employing the lower phase as mobile and the upper phase as stationary. Consecutive separation cycles yielded 1.04 mg of diadinoxanthin with 98% recovery and 93% purity, further increased to >98% after gel permeation purification. A solvent phase formulation strategy reduced solvent use by 1.9% (*n*-heptane), 26% (ethyl acetate), 31% (ethanol), and 37% (water), improving process sustainability. Diadinoxanthin was evaluated along with fucoxanthin and *P. tricornutum* extract against a panel of mediators of cutaneous photoaging and skin carcinogenesis. Diadinoxanthin reduced $^{\bullet}NO$ and $O_2^{\bullet-}$ levels, but was particularly effective against ABTS and DPPH radicals, with EC_{50} and EC_{25} values of 7.41 ± 0.11 μM and 12.21 ± 0.79 μM, respectively. It strongly inhibited 5-lipoxygenase (IC_{50} = 40.10 ± 2.32 μM) and displayed senolytic activity against senescent cancer cells. Compared with fucoxanthin, diadinoxanthin demonstrated superior antiradical, anti-inflammatory and senolytic effects, with slightly lower anti-melanogenic potential. This study establishes an efficient, eco-friendly HPCCC process for the recovery of diadinoxanthin and highlights its value as a quality marker and multifunctional bioactive. The approach offers a scalable model for diatom-based biorefineries producing high-value metabolites with lower solvent use.

1. Introduction

Diatoms are recognized as prolific producers of photosynthetic pigments, particularly carotenoids and chlorophylls [1]. Their carotenoid profile typically includes fucoxanthin, diadinoxanthin, diatoxanthin, and β-carotene, with fucoxanthin being the dominant pigment [1]. Among these, fucoxanthin has received extensive attention due to its diverse biological activities, including strong antioxidant [2–5], anti-obesity and anti-diabetic [6–9], anti-inflammatory [10,11], anticancer [12–14], and neuroprotective effects [2,15]. Diatom-derived extracts are becoming increasingly commercially valuable and marketed as active ingredients for nutraceutical and cosmetic formulations, with their efficacy primarily attributed to fucoxanthin. Several *Phaeodactylum tricornutum*-based products exemplify this trend, including **Fucovital™** (Algatechnologies Ltd., Israel), a dietary supplement standardized to 3% fucoxanthin [16], and **NutriXanthin™** and

* Corresponding author at: Laboratory of Algal Biotechnology – Centre ALGATECH, Institute of Microbiology of the Czech Academy of Sciences, Opatovický mlýn, 379 01, Třeboň, Czech Republic.
E-mail address: jcheel@alga.cz (J. Cheel).

https://doi.org/10.1016/j.algal.2026.104566
Received 5 November 2025; Received in revised form 27 January 2026; Accepted 3 February 2026
Available online 5 February 2026

DermaXanthin™ (Alga-Health, Israel) which serve as fucoxanthin-rich ingredients for food supplements and skincare formulations, respectively [17]. Similarly, **Gamephyt™** and **BrainPhyt™** (Microphyt, France) are marketed for enhancing cognitive performance [18]. Fucoxanthin is consistently labelled in these formulations as the main bioactive component [19]. However, the exclusive emphasis on fucoxanthin overlooks the potential role of other structurally related carotenoids occurring in the same extracts. Among them, diadinoxanthin remains particularly understudied despite being a commonly occurring xanthophyll in diatoms. This knowledge gap suggests that additional bioactive carotenoids, particularly diadinoxanthin, may substantially contribute to or synergize with fucoxanthin-driven biological effects in diatom-derived products. Nevertheless, the lack of scalable isolation methods has so far prevented systematic evaluation and large-scale production of this compound, limiting its translational and industrial exploration.

Diadinoxanthin (Fig. 1a) is a monoepoxy xanthophyll that plays a central role in the diadinoxanthin–diatoxanthin cycle, a key photoprotective mechanism in diatoms [1]. Under high-light conditions, diadinoxanthin is enzymatically de-epoxidized to diatoxanthin, enabling the dissipation of excess excitation energy and protecting cells against photooxidative damage. This intrinsic antioxidant role within the photosynthetic apparatus suggests that diadinoxanthin may also possess significant radical scavenging and cytoprotective activity outside the photosynthetic context. However, despite its structural similarity to fucoxanthin (Fig. 1b), diadinoxanthin has been comparatively understudied, and its biological properties remain poorly characterized [1,20]. Emerging evidence indicates that diadinoxanthin exhibits diverse bioactivities, including antimicrobial effects against Gram-positive bacteria [21] and concentration-dependent antioxidant capacity through DPPH and ABTS radical scavenging [21]. Such effects provide preliminary evidence supporting the use of diadinoxanthin as an active ingredient for incorporation into nutraceutical, cosmetic, and pharmaceutical formulations. However, reports on its bioactive and pharmacological effects remain scarce compared with those available for fucoxanthin and other algae-derived ingredients, particularly on skin disorders and cutaneous aging. Reported isolations rely on labor-intensive workflows such as ODS column chromatography followed by ethanol precipitation [21], multistep extraction–saponification–partitioning–chromatography processes [22], and preparative thin-layer chromatography combined with Al_2O_3 and HPLC purification [20]. While effective for analytical purposes, these techniques are solvent-intensive, time-consuming, and poorly suited for scale-up. Addressing these extraction and purification limitations is crucial for the systematic exploration, valorization, and large-scale production of diadinoxanthin as a high-value bioactive metabolite.

High-performance countercurrent chromatography (HPCCC), a form of liquid-liquid chromatography, represents a powerful alternative for such separations. Unlike traditional solid-phase chromatography, HPCCC relies exclusively on two immiscible liquid phases, eliminating irreversible adsorption, minimizing sample loss, and enhancing compound recovery [23]. The technique operates under a centrifugal field that retains one phase as stationary while the other flows as the mobile phase, enabling highly selective and reproducible partitioning based on solute distribution coefficients [24,25]. Both hydrodynamic (CCC, HSCCC, HPCCC) and hydrostatic (centrifugal partition chromatography, CPC) variants have been successfully applied for pigment isolation from algal biomass. Examples include fucoxanthin recovery from *Laminaria japonica*, *Undaria pinnatifida*, and *Sargassum fusiforme* via HSCCC [26]; fucoxanthin purification from *Eisenia bicyclis* using CPC [27]; and CPC–flash workflows for *Tisochrysis lutea* [28]. More recently, HPCCC has been optimized for the scalable purification of fucoxanthin from *P. tricornutum* [29] and β-carotene from *Dunaliella* sp. [30], underscoring its potential for industrial-scale purification of bioactive algae-derived pigments. Consecutive CCC separations have also been previously reported for the purification of active compounds from higher plants, demonstrating high reproducibility [31,32]. However, no study to date has established an efficient HPCCC workflow specifically tailored for diadinoxanthin isolation, nor integrated it with downstream biological characterization to evaluate its potential as a multifunctional bioactive compound.

The present work is based on the central premise that diadinoxanthin can be isolated through a selective, solvent-efficient HPCCC workflow and that the purified compound possesses biologically relevant activities applicable to skin health and photoaging. To explore this, we developed an HPCCC-guided biorefinery strategy combined with gel permeation chromatography (GPC) for the selective recovery and biofunctional evaluation of diadinoxanthin from *P. tricornutum*. The optimized HPCCC process incorporates a solvent-phase formulation approach to enhance sustainability and reduce solvent consumption. Along with an efficient recovery and purification strategy for obtaining diadinoxanthin, the experimental design of the current study also enables to deliver in vitro

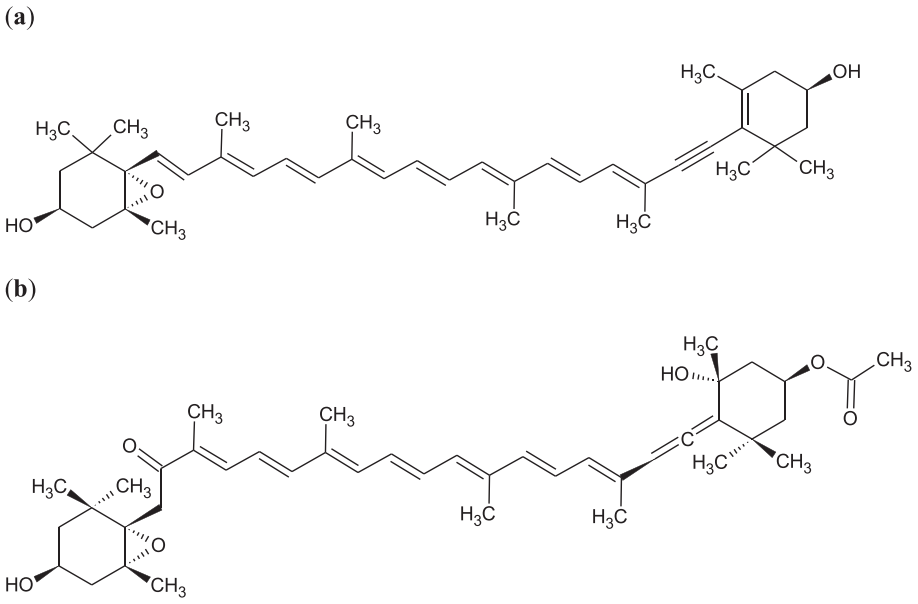

Fig. 1. Chemical structure of diadinoxanthin (**a**) and fucoxanthin (**b**).

cell-free and cell-based data supporting its potential use in cutaneous photoaging and other skin disorders, establishing it as a possible alternative to fucoxanthin for cosmetic and dermopharmaceutical formulations. The isolated compound was evaluated for its antiradical, anti-inflammatory, and anti-melanogenic activities along with its senolytic activity in senescent human melanoma SK-MEL-103 cells, in comparison with fucoxanthin and the crude *P. tricornutum* extract. This integrated approach provides a scalable and environmentally conscious platform for diadinoxanthin isolation and establishes its bioactive profile as a multifunctional carotenoid to be used in skincare and pharmaceutical formulations.

2. Materials and methods

2.1. Microalgae cultivation

The diatom *P. tricornutum* CCAP 1055/5 (Culture Collection of Algae and Protozoa, Scottish Association for Marine Science, UK) was cultivated phototrophically in an 80 L glass tubular photobioreactor. The culture was continuously aerated with an air-CO_2 mixture (98:2, *v/v*) at a flow rate of 5 L min^{-1} to ensure homogenous mixing and prevent sedimentation. Illumination was supplied by a centrally positioned LED daylight lamp delivering 1500 μmol photons m^{-2} s^{-1}, measured with a LI-250 light meter (LI-COR Biosciences, Nebraska, USA) at 3 cm from the light source. Cultivation was carried out in modified Artificial Seawater Medium [33] supplemented with 0.1 M sodium metasilicate (SiO_3) at 20 ± 1 °C. Cells were harvested during the exponential growth phase by centrifugation (Sigma 8KS, Sigma Laborzentrifugen, Germany) at 20,461 ×*g* for 10 min at 4 °C. The collected biomass was immediately frozen at −70 °C and lyophilized for 72 h using a ScanVac CoolSafe freeze dryer (LaboGene ApS, Lynge, Denmark). A total of 100 g of dry biomass was obtained. The corresponding growth curve of *P. tricornutum* is shown in **Supplementary Material** Fig. S1.

2.2. Optimization of biomass extraction

To produce diadinoxanthin-enriched extract from *P. tricornutum* biomass, two extraction strategies were assessed: ultrasound-assisted extraction (UAE) and mortar-and-pestle-assisted extraction (MPE). A range of solvents was evaluated, including absolute ethanol, 80% ethanol (AnalaR Normapur, VWR Inc., France), acetone, methanol (HiPerSolv Chromanorm, VWR Inc., France), ethyl acetate, *n*-heptane (HiPerSolv Chromanorm, VWR Inc., Poland), as well as the upper and lower phases of the selected solvent system. In each trial, 10 mg of dried biomass was extracted with 5 mL of the selected solvent. UAE experiments were carried out for 30 min in an ultrasonic bath (K6 Kraintek, Slovakia) operating at 38 kHz and 47.77 W•cm^{-2} at 25 °C. Diadinoxanthin content in the extracts was quantified by high-performance liquid chromatography coupled with diode array detection (HPLC-DAD). The most effective extraction system was subsequently employed for the large-scale production of a diadinoxanthin-rich extract, from which diadinoxanthin was isolated using HPCCC.

2.3. High performance countercurrent chromatography (HPCCC) separation

2.3.1. Apparatus

The produced extract of *P. tricornutum* was subjected to HPCCC (Spectrum, Dynamic Extractions Ltd., Slough, UK) to obtain diadinoxanthin. The separation was performed in a 134 mL PTFE coil (3.2 mm i.d.) operated under controlled rotation, with temperature stabilization by a Smart Water Chiller H50/H150 (LabTech Srl, Sorisole Bergamo, Italy). The mobile phase was pumped by a Q-Grad pump system (LabAlliance, State College, PA, USA). The elution of the target compound was continuously monitored at 440 nm using a Sapphire UV-VIS spectrophotometer (ECOM spol. s r.o., Prague, Czech Republic), and the chromatographic profiles were recorded and processed using EZChrom SI software (v.3.3.2 SP2, Agilent Technologies, Pleasanton, CA, USA).

2.3.2. Design of the biphasic solvent system for HPCCC

Efficient separation in HPCCC strongly depends on the choice of the biphasic solvent system. In order to find suitable conditions for the isolation of the target compound from the extract of *P. tricornutum*, solvent mixtures were prepared and evaluated. The selection was based on three important physicochemical parameters: a partition coefficient (*K*) between 0.5 and 3.5 [34,35], a settling time below 30 s, and a density difference between the phases of more than 0.08 g mL^{-1} [36]. The solvent systems were prepared with *n*-heptane, ethanol, ethyl acetate, and deionized water in different proportions (Table 1). An optimal system was defined as one that fulfills all of the above physicochemical criteria [34–36]. Partition coefficients were determined by dissolving 2 mg of *P. tricornutum* extract in 2 mL of the equilibrated biphasic mixture (1 mL of each phase). After shaking and 10 min of phase separation, aliquots from both layers were transferred to HPLC vials and analyzed by HPLC-DAD. The *K* values were calculated as the ratio of the peak area of the target substance in the upper to the lower phase. Settling time was determined by mixing 2 mL of each phase in a test tube, inverting three times, and recording the time to complete phase separation [35]. The volume ratios of the phases were determined after equilibration, and the density differences were measured by weighing 1 mL of each phase with a microbalance [35].

2.3.3. HPCCC separation procedure

Based on the results presented in Table 1, the solvent system 1 was chosen for the separation of diadinoxanthin and subsequently applied to the HPCCC apparatus. The separation conditions were first optimized on the analytical coil (24 mL) of the instrument to achieve maximum efficiency and sample processing capacity. After establishing the optimal parameters (sample loadings and mobile phase flow rate), the procedure was scaled up using the semi-preparative coil (134 mL). To prepare the instrument, the stationary phase (upper phase) was introduced into the column at a flow rate of 5 mL min^{-1} until two full column volumes were loaded. Once filling was complete, the rotation was initiated at 1600 rpm. The mobile phase (lower phase) was then introduced at 30 °C and continued until hydrodynamic equilibrium was established, confirmed by the emergence of the mobile phase without displacement of the stationary phase. The sample solution consisted of *P. tricornutum* extract dissolved in one volume of the mobile phase. Fractions were collected manually and analyzed by HPLC-DAD.

The retention of the stationary phase (*Sf*) was calculated using the following formula:

$$Sf\ (\%) = \frac{Vs}{Vc} \times 100 \tag{1}$$

where *Vc* denotes the total volume of the HPCCC column, and Vs corresponds to the volume of stationary phase remaining within the column after hydrodynamic equilibrium has been reached [37].

The retention time (t_R) of the target compound was calculated following the procedure previously described, using the equation below:

$$t_R = \frac{V_M + (K \times V_S)}{F} \tag{2}$$

where V_M is the volume of the mobile phase at hydrodynamic equilibrium, *K* represents the partition coefficient of the target compound, V_S is the volume of the stationary phase at hydrodynamic equilibrium, and *F* denotes the mobile phase flow rate [37].

The retention volume (V_R) of the target compound in the HPCCC separation was calculated as follows:

$$V_R = t_R \times F \tag{3}$$

where t_R corresponds to the elution (retention) time of the target

Table 1
Partition coefficients, settling times, and density differences of biphasic solvent systems evaluated for diadinoxanthin.

Solvent Systems	Composition	Relative proportions of solvents (*v/v/v/v*)	Phase Volume ratio (UP/LP)	Settling time (s)	Density difference (LP − UP, g mL $^{-1}$)	Partition coefficient (*K*) of diadinoxanthin
1	*n*-Hep/EtOAc/EtOH/H_2O	5/4/5/3	0.67	15	0.1451	1.8
2	*n*-Hep/EtOAc/EtOH/H_2O	5/5/5/3	0.73	20	0.1317	3.0
3	*n*-Hep/EtOAc/EtOH/H_2O	5/6/5/3	0.79	26	0.1014	3.8
4	*n*-Hep/EtOAc/EtOH/H_2O	5/5/5/5	0.72	30	0.1273	10.6
5	*n*-Hep/EtOAc/EtOH/H_2O	5/5/6/5	0.57	21	0.1445	6.1
6	*n*-Hep/EtOAc/EtOH/H_2O	5/5/6/4	0.59	18	0.1301	4.2
7	*n*-Hep/EtOAc/EtOH/H_2O	5/5/6/3	0.58	17	0.1239	0.8
8	*n*-Hep/EtOAc/EtOH/H_2O	5/5/7/3	0.43	15	0.1212	0.7
9	*n*-Hep/EtOAc/EtOH/H_2O	5/5/8/3	0.36	19	0.1268	0.3

n-hep: *n*-heptane. EtOAc: ethyl acetate. EtOH: ethanol. UP: upper phase. LP: lower phase.

compound obtained during the chromatographic run, while *F* refers to the flow rate of the mobile phase applied throughout the process [38].

2.3.4. Determination of phase composition by proton nuclear magnetic resonance (^{1}H NMR)

The chemical composition of both the upper and lower phases from the selected biphasic solvent system was characterized using ^{1}H NMR spectroscopy. For each phase, 550 μL of the liquid sample was transferred into a short NMR tube (103.5 mm in length, 5 mm in outer diameter). To ensure proper frequency locking and minimize interference from residual water signals, a sealed insert made from a 1.7 mm NMR tube containing 80 μL of C_6D_6 was positioned at the center of the 5 mm tube. Spectra were collected using a Bruker AVANCE III 600 MHz spectrometer equipped with a TCI cryoprobe and a SampleJet autosampler, controlled by TopSpin 3.5 software (Bruker Biospin GmbH, Rheinstetten, Germany). Measurements were automated via ICON-NMR. The ^{1}H NMR spectra were acquired under ^{13}C-decoupling conditions using the zgpg30 pulse program, where decoupling was applied only during acquisition to minimize temperature-induced magnetic field drifts. Experimental parameters included a relaxation delay (D_1) of 60 s, 16 scans, and a temperature of 20 °C. Data processing involved zero-filling to four times the original data points and applying a 0.3 Hz line-broadening factor prior to Fourier transformation to enhance spectral quality and reduce noise. Peak integration was performed in TopSpin 3.5, with baseline correction algorithms that account for local slope and bias variations. The resulting relative peak integrals were used to calculate and estimate the molar ratios of solvents in each phase. From these ratios, the proportional volume (V_P) of each solvent in the upper and lower layers was calculated as follows:

$$V_P = \frac{n \times M}{D} \quad (4)$$

where *n* represents the relative molar fraction of each solvent, as determined from ^{1}H NMR (Table 2), *M* is the molar mass, and *D* is the density of the solvent at 298 K. The molar masses (g mol^{-1}) of *n*-heptane, ethyl acetate, ethanol and water were 100.205, 88.106, 46.069, and 18.015, respectively, and their corresponding densities (g mL^{-1}) were 0.684, 0.902, 0.789, and 0.997. These calculated values provided a quantitative description of the solvent distribution between the two liquid phases, enabling assessment of the phase equilibrium characteristics of the chosen biphasic system.

Table 2
Molar composition of individual solvents in the upper (UP) and lower (LP) phases of the selected biphasic solvent system (System 1: *n*-heptane/ethyl acetate/ethanol/water, 5:4:5:3, *v/v/v/v*), as determined by ^{1}H NMR analysis.

System	Liquid phases	Molar proportions (*n*)			
		n-heptane	ethyl acetate	ethanol	water
1	UP	0.563	0.255	0.129	0.054
	LP	0.002	0.091	0.304	0.602

2.4. Final purification of diadinoxanthin via gel permeation chromatography

Following HPCCC separation, diadinoxanthin fraction was subjected to further purification using gel permeation chromatography. The procedure employed an open glass column (30 cm × 4 cm i.d.) packed with Sephadex LH-20. Methanol (100%) was used as the eluent, at a steady flow rate of 0.5 mL min^{-1}. The elution of diadinoxanthin was visually tracked, and the relevant fractions were combined. Pooled fractions were then concentrated under reduced pressure at 28 °C using a rotary evaporator to obtain purified diadinoxanthin.

2.5. HPLC-DAD analysis and quantification

The diadinoxanthin obtained from HPCCC and crude extract of *P. tricornutum* were subjected to chromatographic profiling on a HPLC system (Agilent 1260 Series, Santa Clara, CA, USA) equipped with a diode array detector. Separation was achieved on a reversed-phase Luna® C8 column (100 × 4.6 mm, 3 μm, 100 Å) maintained at 30 °C. Elution was carried out at 0.8 mL min^{-1} with a binary solvent system composed of water (solvent A) and methanol (solvent B), using the following gradient program: 0–20 min, 20% to 0% A; 20–25 min, 0% A; 25–27 min, 0% to 20% A; 27–30 min, 20% A. Chromatograms were recorded at 440 nm. Quantitative analysis of diadinoxanthin was performed against a commercial reference standard (Sigma Aldrich, Darmstadt, Germany). Calibration was established with five standard concentrations ranging from 0.48 to 31.25 μg mL^{-1} with an injection volume of 20 μL. The resulting regression equation was $y = 159.81\times + 2.901$ ($R^2 = 1$), where x represents diadinoxanthin concentration (μg mL^{-1}) and y is the corresponding peak area. This calibration model was also applied to assess the purity of the isolated diadinoxanthin.

2.6. Confirmation of chemical identity of isolated compound

The structural identity of the isolated compound was established using a Dionex UltiMate 3000 HPLC system (Thermo Scientific, Carlsbad, CA, USA) connected to a high-resolution tandem mass spectrometer (HRMS/MS, Impact HD, Bruker, Billerica, MA, USA) equipped with an atmospheric pressure chemical ionization (APCI) interface operating in positive ion mode. To enhance ion formation, 0.1% formic acid was incorporated into both mobile phases. Mass spectrometric conditions were adjusted as follows: capillary potential 2500 V, nitrogen drying stream at 5 L min^{-1}, drying temperature 350 °C, vaporizer 450 °C, and nebulizer pressure 20 psi. Data acquisition was carried out in full-scan mode across an *m/z* window of 100–2000. Fragmentation of diadinoxanthin was performed with nitrogen as the collision medium and an energy setting of 35 eV. Compound annotation was supported by comparison with previously reported spectral data. Chromatographic details are described in section **2.5**.

2.7. Biological assays

2.7.1. DPPH free radical scavenging activity

The scavenging activity against the radical DPPH (2,2-diphenyl-1-picrylhydrazyl) was evaluated based on the decrease in absorbance of a methanolic DPPH solution, as described previously [39]. Test solutions were prepared at concentrations ranging from 3.125 to 100 μM for diadinoxanthin and 31.25 to 1000 μg mL^{-1} for the algal extract. A commercial fucoxanthin standard (Sigma-Aldrich, Darmstadt, Germany) was used for comparative analysis and quercetin was used as a positive control. Reduction in radical absorbance was monitored spectrophotometrically at 517 nm, with untreated DPPH serving as the reference. The loss of color intensity reflects the ability of the compound to neutralize the free radical. The results are expressed as the percentage of DPPH levels.

2.7.2. ABTS free radical scavenging activity

The antiradical activity against 2,2′-azino-bis-(3-ethylbenzothiazoline-6-sulfonic acid) (ABTS) was evaluated using the ABTS radical cation ($ABTS^{\bullet+}$) decolorization assay, following the procedure previously described [40] with minor modifications. The $ABTS^{\bullet+}$ solution was prepared by mixing 3.5 mM ABTS diammonium salt (Thermo Fisher GmbH, Kandel, Germany) with 1.225 mM potassium persulfate (VWR Inc., Leuven, Belgium) and allowing the reaction to proceed overnight at 30 °C in the dark. Prior to analysis, the resulting stock solution was diluted with absolute ethanol (AnalaR Normapur, VWR Inc., Fontenay-sous-Bois, France) to obtain an absorbance of approximately 0.70 ± 0.02 at 734 nm. For each assay, 225 μL of the diluted $ABTS^{\bullet+}$ solution was mixed with 75 μL of sample solution and incubated for 60 min at 30 °C. The decrease in absorbance was recorded at 734 nm using ethanol as the blank. Test solutions were prepared in ethanol at concentrations ranging from 3.125 to 100 μM for diadinoxanthin and 31.25 to 1000 μg mL^{-1} for the extract. A commercial fucoxanthin standard (Sigma-Aldrich, Darmstadt, Germany) was used for comparison purposes and quercetin was used as a positive control. A control sample containing only $ABTS^{\bullet+}$ and ethanol was measured to ensure stability of the radical solution. The results are expressed as the percentage of $ABTS^{\bullet+}$ levels.

2.7.3. Nitric oxide radical scavenging assay

The scavenging capacity against the nitric oxide radical ($^{\bullet}NO$) was assessed using the Griess colorimetric method [41]. In this assay, 100 μL of each sample solution, prepared at concentrations ranging from 3.125 to 100 μM for diadinoxanthin and 31.25 to 1000 μg mL^{-1} for the algal extract, was mixed with 100 μL of sodium nitroprusside (20 mM) and incubated for 1 h at room temperature under light exposure. After incubation, 100 μL of Griess reagent (composed of 1% sulphanilamide and 0.1% *N*-(1-naphthyl)ethylenediamine dihydrochloride in 2% phosphoric acid) was added. The mixtures were then maintained in the dark for 10 min at room temperature before measurement. A commercial fucoxanthin standard was used for comparative analysis and quercetin was used as a positive control. Absorbance values were recorded at 560 nm, and the results are expressed as the percentage of $^{\bullet}NO$ levels.

2.7.4. Superoxide radical scavenging activity

Superoxide anion radicals ($O_2^{\bullet-}$) were produced through the NADH–PMS reaction system, as previously described [41]. The assay was carried out in a 96-well microplate by combining 50 μL of the sample with 50 μL of NADH (166 μM), 150 μL of nitro blue tetrazolium chloride (NBT) (43 μM), and 50 μL of phenazine methosulfate (PMS) (2.7 μM). The absorbance was measured at 560 nm after 2 min. Test samples were assayed at concentrations of 3.125–100 μM for diadinoxanthin and 31.25–1000 μg mL^{-1} for the algal extract. Fucoxanthin (Sigma-Aldrich, Darmstadt, Germany) was used for comparative analysis and quercetin was used as positive control. The results are expressed as the percentage of $O_2^{\bullet-}$ levels.

2.7.5. Assessment of 5-lipoxygenase enzymatic activity

The inhibitory effects on 5-lipoxygenase (5-LOX) were evaluated by following the generation of conjugated dienes from linoleic acid [41]. For the assay, 20 μL of the test sample, prepared at concentrations ranging from 3.125 to 100 μM for diadinoxanthin and 31.25 to 1000 μg mL^{-1} for the algal extract, was dispensed into a 96-well microplate and combined with 200 μL of sodium phosphate buffer (100 mM, pH 9.0) and 20 μL of soybean-derived 5-LOX (EC 1.13.11.12; 100 U per 20 μL). The enzymatic reaction was triggered by adding 20 μL of linoleic acid solution (4.18 mM in ethanol). Absorbance changes at 234 nm, corresponding to diene formation, were continuously recorded for 3 min to quantify enzyme activity. A commercially available fucoxanthin standard was employed for comparative evaluation at the same concentration range as diadinoxanthin, with quercetin being used as a positive control. Data are expressed as mean ± SEM from three independent experiments performed in triplicate.

2.7.6. Tyrosinase inhibition assay

The effects of diadinoxanthin on tyrosinase activity were assessed using a modified dopachrome formation method [42]. In each well of a 96-well microplate, 40 μL of sample was combined with 80 μL of phosphate buffer (0.05 M, pH 6.8), 40 μL of mushroom tyrosinase (EC 1.14.18.1; 90 U mL^{-1}), and 40 μL of L-DOPA substrate (0.85 μM). The reaction was monitored spectrophotometrically at 475 nm for 3 min, and enzyme inhibition was calculated from the recorded kinetics. A commercial fucoxanthin standard was used for comparative analysis and kojic acid was used as positive control. Data are expressed as mean ± SEM from three independent experiments performed in triplicate.

2.7.7. Senolytic activity

The senolytic activity was evaluated using an in vitro high-throughput screening platform with a Palbociclib-induced senescent melanoma cell line (SK-MEL-103) [43]. Proliferating cells (1000 cells per well) and senescent cells (2000 cells per well) were seeded in white 384-well microplates (Greiner Bio-One) at 60 μL per well. After 24 h, 20 μL of sample solution (triplicate) was added to achieve final concentrations of 88, 176, and 264 μM. DMSO (0.1%) served as a negative control. Plates were incubated at 37 °C for 48 h, followed by the addition of 25 μL ATPlite One Step Reagent (PerkinElmer, Cat. No. 6016731) to determine viability compared to DMSO. The differences in viability between proliferating and senescent cells were compared. A commercial fucoxanthin standard was used for comparative analysis.

2.8. Statistical analysis

Statistical analyses were performed using GraphPad Prism 8.4.2 (GraphPad Software, San Diego, CA, USA). Data normality was verified using the Shapiro–Wilk test. When data met the assumptions of normality, differences between treatment and control groups were analyzed by one-way ANOVA followed by Welch's post hoc test. Statistical significance was set at $p < 0.05$. The number of independent experiments and biological replicates is provided in each figure legend.

3. Results and discussion

3.1. Extract preparation

Efficient purification of intracellular pigments such as diadinoxanthin requires a well-optimized extraction step prior to chromatographic isolation. Extraction solvents are often chemically distinct from those used in liquid-liquid separation systems; however, aligning their composition can improve recovery and simplify downstream processing [29,44]. To explore this concept, the upper (UP1) and lower (LP1) phases of the biphasic solvent system later applied in HPCCC separations (Table 1) were assessed for their ability to extract diadinoxanthin from *P. tricornutum* biomass. Their extraction performance was compared

with that of standard solvents typically employed for microalgal pigment recovery (Fig. 2). Extractions were performed using either ultrasound-assisted extraction (UAE; 30 min) or a mortar-and-pestle-assisted extraction (MPE) approach. Both solvent composition and extraction technique markedly affected diadinoxanthin yield. Among all treatments, the LP1 phase and 80% ethanol produced the highest recoveries, with UAE consistently outperforming mechanical extraction. Previous optimization [21] reported a maximum diadinoxanthin yield of 1.82 mg g^{-1} dry biomass under extraction with 80% ethanol at 25 °C for 120 min (liquid-to-solid ratio 1:40, repeated twice). Diadinoxanthin was also detected in *Tribonema* cf. *minus* biomass extracted by UAE with 80% ethanol, with concentrations ranging from 0.02 to 1.22 mg g^{-1} dry biomass across three cultivation trials [45]. In the present study, UAE using 80% ethanol and LP1 achieved comparable results, yielding 1.40 mg g^{-1} and 1.39 mg g^{-1} diadinoxanthin, respectively. MPE yielded slightly lower values (1.21 mg g^{-1} for ethanol and 1.39 mg g^{-1} for LP1). The LP1 phase demonstrated selective extraction behavior, recovering diadinoxanthin efficiently while limiting the co-extraction of highly lipophilic pigments and impurities. This compositional selectivity is advantageous for subsequent HPCCC purification, reducing solvent use and simplifying phase equilibration. Based on extraction efficiency and selectivity, UAE with LP1 for 30 min was selected as the large-scale method. Using this optimized protocol, 10 g of dried *P. tricornutum* biomass extracted with 1.5 L of LP1 yielded 3.48 g of dried extract. This corresponded to three successive extractions using 0.5 L LP1 each, resulting in a final combined extract volume of 1.5 L of LP1. This protocol maintained extraction performance comparable to previous small-scale studies and to our earlier work using 1.2 L of solvent per equivalent biomass [29]. The resulting extract was subsequently used as the feed material for HPCCC-based separation of diadinoxanthin.

3.2. Analytical-scale HPCCC method development and scale-up to semi-preparative separation

To establish an efficient HPCCC separation protocol for diadinoxanthin, several biphasic solvent systems were developed by varying the volumetric ratios of *n*-heptane, ethyl acetate, ethanol, and water (Table 1). The initial composition (5:5:5:5, *v/v/v/v*) was selected from the Arizona solvent system library [46] and subsequently modified to optimize phase polarity and solute partitioning behavior. For the development of biphasic solvent systems, particular attention was given to regulatory compliance with food, cosmetic, and pharmaceutical standards to ensure the suitability of the proposed process for future industrial applications. Ethanol and ethyl acetate are authorized extraction solvents for the production of foodstuffs and food ingredients, while hexane is permitted provided that its residual level in the final product does not exceed 1 mg kg^{-1} [47]. In this study, *n*-heptane was selected as a less toxic and more environmentally compatible alternative to hexane [48]. According to EMA and FDA guidelines [49,50], the residual content of *n*-heptane, ethyl acetate, and ethanol in pharmaceutical excipients or active substances should remain below 5000 ppm. These solvents are also accepted for use in cosmetic formulations [51]. Such limits can be reliably achieved through standard solvent removal during the final drying stage, ensuring that the developed solvent system aligns with regulatory safety requirements across multiple product categories.

A biphasic solvent system suitable for HPCCC must exhibit both an appropriate partition coefficient ($K = 0.5–3.5$) for the target compound and stable stationary phase retention, supported by a density difference above 0.08 g mL^{-1} and a phase settling time below 30 s [23,34,36]. Among the tested systems, the composition *n*-heptane-ethyl acetate-ethanol-water (5:4:5:3, *v/v/v/v*) (Table 1) provided the most favorable balance of these properties and was selected for further optimization.

Analytical-scale separations were performed using a 24 mL HPCCC coil in reverse-phase mode, with the lower phase as the mobile phase and the upper phase as the stationary phase. Key operational parameters such as mobile phase flow rate and sample load were optimized while maintaining constant conditions for rotational speed (1600 rpm), injection loop volume (0.5 mL), and temperature (30 °C). Optimal resolution and stationary phase retention were obtained at 0.5 mL min^{-1} and 20 mg sample load (Fig. 3; Table 3), which yielded the highest purity of diadinoxanthin under hydrodynamic equilibrium. The scale-up of the HPCCC procedure from the analytical to the semi-preparative level was conducted using a linear scaling approach previously outlined [52]. To ensure comparable hydrodynamic conditions, the centrifugal field ("g" force) was kept constant in both column configurations. The semi-preparative coil (134 mL) possessed roughly six times the volume of the analytical column (24 mL), and the maximum rotational speed of 1600 rpm was applied in both cases. Scaling was performed proportionally to the column volume ratio. Thus, the sample load, mobile phase flow rate, and injection loop volume were increased to 120 mg, 3 mL min^{-1}, and 3 mL, respectively, each representing a sixfold increase relative to the analytical setup. Under these conditions, the stationary phase retention (*Sf*) reached 32.8% by the end of the process, and diadinoxanthin eluted at approximately 50 min, yielding 0.52 mg of purified product at 93% purity (Fig. 4a). A control experiment using a

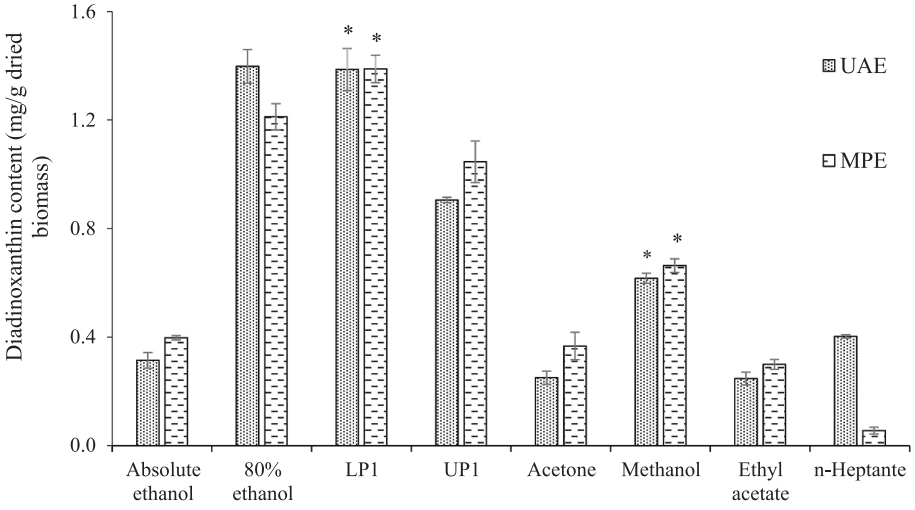

Fig. 2. Comparison of extraction methods for diadinoxanthin recovery from *Phaeodactylum tricornutum*. Extraction was compared between ultrasound-assisted extraction (UAE, 30 min) and mortar-and-pestle extraction (MPE) with organic solvent as well as upper (UP1) and lower (LP1) phases of the selected biphasic solvent system 1. Data represent mean ± SD ($n = 3$). Bars with identical symbols (*) are not significantly different ($p < 0.05$).

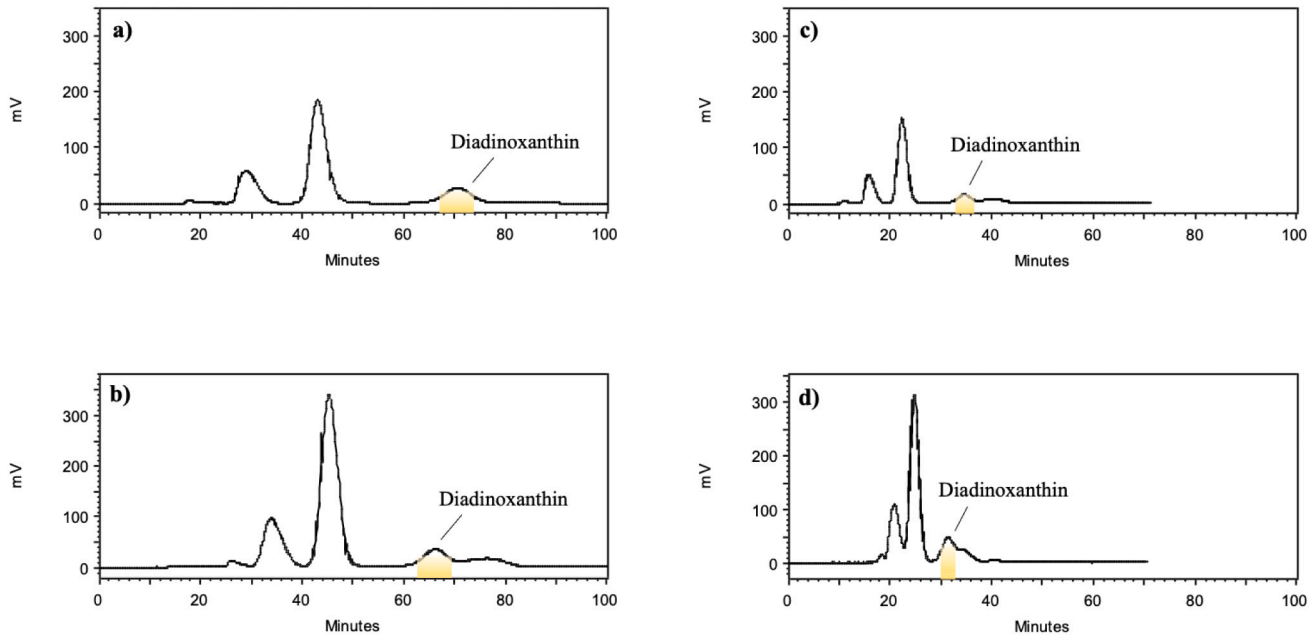

Fig. 3. Optimization of HPCCC parameters for the isolation of diadinoxanthin from *Phaeodactylum tricornutum* extract. Chromatographic performance was evaluated under varying sample loadings and mobile-phase flow rates: (**a**) 20 mg at 0.5 mL min^{-1}, (**b**) 40 mg at 0.5 mL min^{-1}, (**c**) 20 mg at 1.0 mL min^{-1}, and (**d**) 40 mg at 1.0 mL min^{-1}. The biphasic solvent system (System 1) comprised *n*-heptane, ethyl acetate, ethanol, and water (5:4:5:3, *v/v/v/v*). Separations were performed in reverse elution mode using the lower phase as mobile phase. Samples were dissolved in 0.5 mL of the mobile phase and injected via a 0.5 mL sample loop. The column temperature was maintained at 30 °C, and elution was monitored at 440 nm.

Table 3
Effect of sample load and mobile phase flow rate on stationary phase retention and resolution during HPCCC separation of diadinoxanthin from *Phaeodactylum tricornutum*. Experiments were performed in the analytical coil (24 mL) using a biphasic solvent system composed of *n*-heptane, ethyl acetate, ethanol, and water (5:4:5:3, *v/v/v/v*) under reverse elution mode, with the lower phase as the mobile phase. Column temperature was maintained at 30°C, and detection was set at 440 nm. Samples were dissolved in 0.5 mL of mobile phase and introduced via a 0.5 mL injection loop.

Optimization experiments	Flow rate (mL min^{-1})	*Sf* at the hydrodynamic equilibrium in HPCCC (%)	Loading per injection (mg)	Peak Resolution (1/2)	*Sf* at the end of the HPCCC separation run (%)	Peak Purity (%)
a	0.5	60.42	20	1.53	56.25	95
b	0.5	60.42	40	1.20	39.58	86
c	1.0	45.83	20	1.30	41.66	88
d	1.0	45.83	40	0.73	14.58	63

Rt: Retention time. The peak resolution was calculated as follows: Rs = 2(Rt2-Rt1)/(W2 + W1), where 1 corresponds to diadinoxanthin and 2 is the contaminant peak. W: the peak width at base. **a** (Rt1 = 71 min, Rt2 = 84 min and W1 ~ 6, W2 ~ 11). **b** (Rt1 = 68 min, Rt2 = 77 min and W1 ~ 6, W2 ~ 9). **c** (Rt1 = 34.8 min, Rt2 = 40.8 min and W1 ~ 3.6, W2 ~ 5.6). **d** (Rt1 = 31.7 min, Rt2 = 34 min and W1 ~ 2.4, W2 ~ 3.9).

reduced injection loop (1 mL) led to lower stationary phase retention by the end of the process (*Sf* ≈ 22%) and diminished chromatographic resolution (Fig. 4b). This decline likely resulted from stationary phase disruption caused by increased sample concentration, emphasizing the importance of maintaining hydrodynamic stability during scale-up. Consequently, a 3 mL injection loop was selected for subsequent separations. The theoretical retention time (t_R) of diadinoxanthin, estimated using its partition coefficient and stationary phase retention (**Eq. 2**) [24,37], was 56 min, closely aligning with the experimentally observed elution at 50 min. The minor deviation likely reflects gradual stationary phase displacement during operation, a common feature of HPCCC separations [29]. The calculation of the theoretical retention time (t_R) is of particular interest for calculating a priori the separation process duration and the solvent consumption, which are critical parameters when further increasing process scale. The partition coefficient (*K*) of diadinoxanthin during CCC was determined as 1.4 based on the experimental elution profile and **Eq. 2**, compared with a *K* value of 1.8 obtained from HPLC measurements (Table 1). The slight discrepancy is expected, as HPLC-derived *K* values reflect static partitioning under equilibrium, whereas CCC operates under dynamic conditions with continuous mobile-phase flow and centrifugal forces, which can slightly alter solute distribution. Despite this, the observed *K* value was sufficient to achieve efficient and reproducible separation, confirming the suitability of the selected biphasic solvent system.

3.3. Sequential two-cycle HPCCC for diadinoxanthin separation

A two-cycle HPCCC protocol was developed to enhance process productivity and recovery of diadinoxanthin. The solvent system used (**System 1**) exhibited a phase volume ratio of 0.67 (Table 1), which, if prepared conventionally, generates mismatched phase volumes and solvent waste. To prevent this, both phases were individually formulated using *n*-heptane, ethyl acetate, ethanol, and water at volume ratios of 7.117:2.149:0.650:0.084 and 0.077:2.351:4.695:2.877 (*v/v/v/v*) for the upper and lower phases, respectively. These formulations were derived from ^{1}H NMR compositional data (Table 2) and physicochemical properties of the solvents using **Eq. 4**. The partition coefficient and density difference of the resulting formulated liquid phases closely matched those of the conventional biphasic mixture, confirming its suitability for HPCCC operation. The retention time of diadinoxanthin was calculated prior to its separation to estimate solvent requirements. Using **Eqs. 2** and **3**, the predicted retention time and elution volume for diadinoxanthin

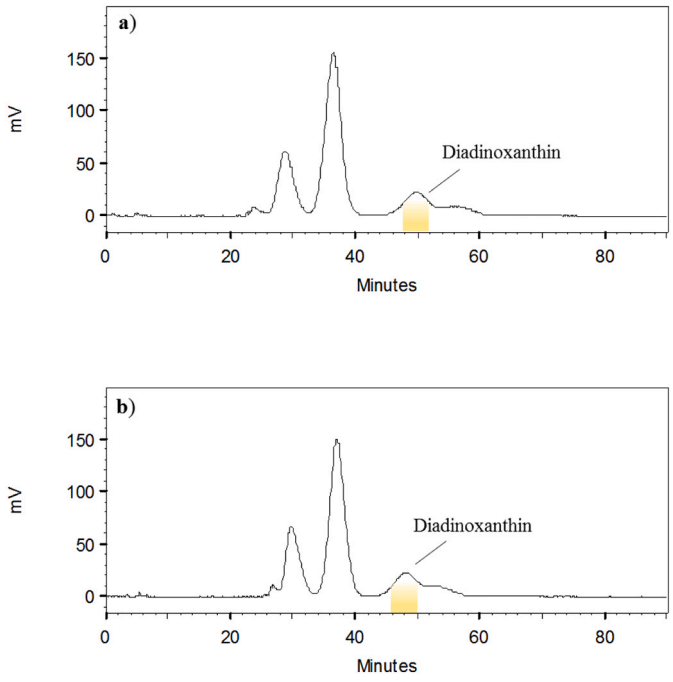

Fig. 4. Scale-up of HPCCC for preparative isolation of diadinoxanthin from *Phaeodactylum tricornutum* extract. A biphasic solvent system (System 1: *n*-heptane, ethyl acetate, ethanol, and water, 5:4:5:3, *v/v/v/v*) was used. Each injection contained 120 mg of extract dissolved in the mobile phase. Chromatograms show (**a**) 3 mL loop and (**b**) 1 mL loop, both at a mobile phase flow rate of 3 mL min^{-1}. HPCCC conditions: 1600 rpm, 30 °C, detection at 440 nm.

were 56.4 min and 169.2 mL, respectively. Accordingly, 169.2 mL of mobile phase (lower phase) and 250 mL of stationary phase (corresponding to more than one column volume) were secured for each complete run. These values represented the minimum volumes required for the separation process, excluding the additional volume associated with hydrodynamic equilibrium. The separation was performed in two consecutive cycles under optimized conditions (Fig. 5). After each elution of the target compound in the first separation cycle, the system was regenerated through stationary-phase extrusion, switching the flow from mobile to stationary phase while maintaining column rotation [29,53]. This step removed residual solutes, reloaded the column with fresh stationary phase, and restored hydrodynamic equilibrium before the next sample injection. Each cycle processed 120 mg of *P. tricornutum* extract, for a total of 240 mg. The overall operation lasted 185 min and consisted of column filling with the upper phase (25 min, 10 mL min^{-1}), equilibration with the lower phase (15 min, 3 mL min^{-1}), two elution cycles (55 min each), and stationary-phase extrusion (20 min) followed by re-equilibration (15 min). Across both cycles, the process yielded 1.04 mg of diadinoxanthin with a purity of 93%. Considering the pigment content in the crude extract (4.09 mg g^{-1} dry extract), the recovery efficiency of the HPCCC process reached 98%. HPLC-DAD chromatograms of the algal extract and separated diadinoxanthin (Fig. 6a,b,c) demonstrate the selectivity and efficiency of the developed separation method. Overall, the use of formulated liquid phases reduced total solvent consumption to 870 mL (450 mL upper phase and 420 mL lower phase), corresponding to savings of 1.9%, 26%, 31%, and 37% in *n*-heptane, ethyl acetate, ethanol, and water, respectively, compared with non-formulated systems (Table 4). This approach provides a reliable and resource-efficient strategy for the preparative separation of diadinoxanthin from *P. tricornutum* biomass. Although the amount of diadinoxanthin obtained in this study (1.04 mg) may appear limited, it primarily reflects the low intracellular abundance of this minor carotenoid in *P. tricornutum* under the applied cultivation conditions rather than a limitation of the separation method itself. The two-cycle HPCCC protocol demonstrated here confirms the robustness, high recovery, and scalability of the developed method, as evidenced by the successful volumetric scale-up from an analytical (24 mL) to a semi-preparative (134 mL) column without loss of separation performance. Based on the experimental data generated in this work, a theoretical throughput estimation for larger available CCC systems [29] was conducted (Table 5). These projections indicate that a pilot-scale CCC unit with an 18 L column volume could achieve production levels of approximately 1 g of diadinoxanthin within 24 h of continuous operation per week, provided sufficient extract availability. Further increases in productivity may be achieved through upstream optimization strategies, including refining cultivation conditions and using metabolic engineering approaches to enhance diadinoxanthin cellular content. Together, these results highlight the strong potential of HPCCC as a downstream platform for the large scale production of diadinoxanthin.

3.4. Final purification

The diadinoxanthin-enriched fraction obtained after HPCCC separation was subsequently purified via gel permeation chromatography (GPC). For this step, an open glass column (30 cm × 4 cm i.d.) was packed with Sephadex LH-20. Methanol (100%) served as the eluent at a flow rate of 0.5 mL min^{-1}. The progression of diadinoxanthin through the column was tracked visually, and the relevant fraction was collected. This fraction was then concentrated under reduced pressure at 28 °C using a rotary evaporator, resulting in a final yield of 0.95 mg of purified diadinoxanthin.

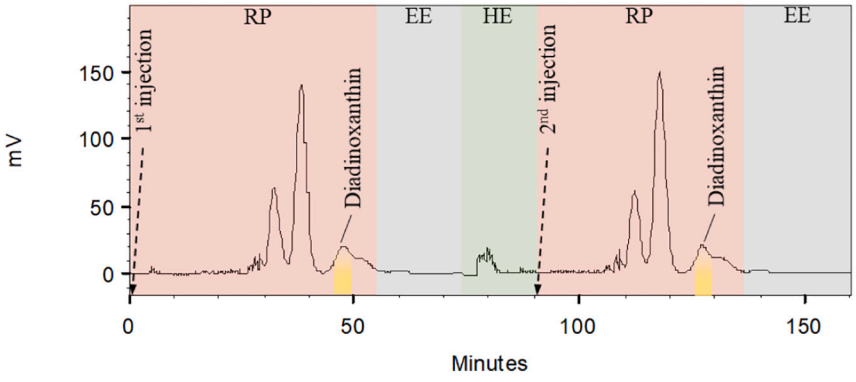

Fig. 5. Sequential two-cycle HPCCC process for separation of diadinoxanthin from *Phaeodactylum tricornutum* extract. Separation was performed using a biphasic solvent system (System 1: *n*-heptane, ethyl acetate, ethanol, and water, 5:4:5:3, *v/v/v/v*). Each injection contained 120 mg of extract dissolved in 3 mL of the mobile phase (3 mL loop). Operating conditions: flow rate 3 mL min^{-1}, rotational speed 1600 rpm, column temperature 30 °C, and detection at 440 nm.

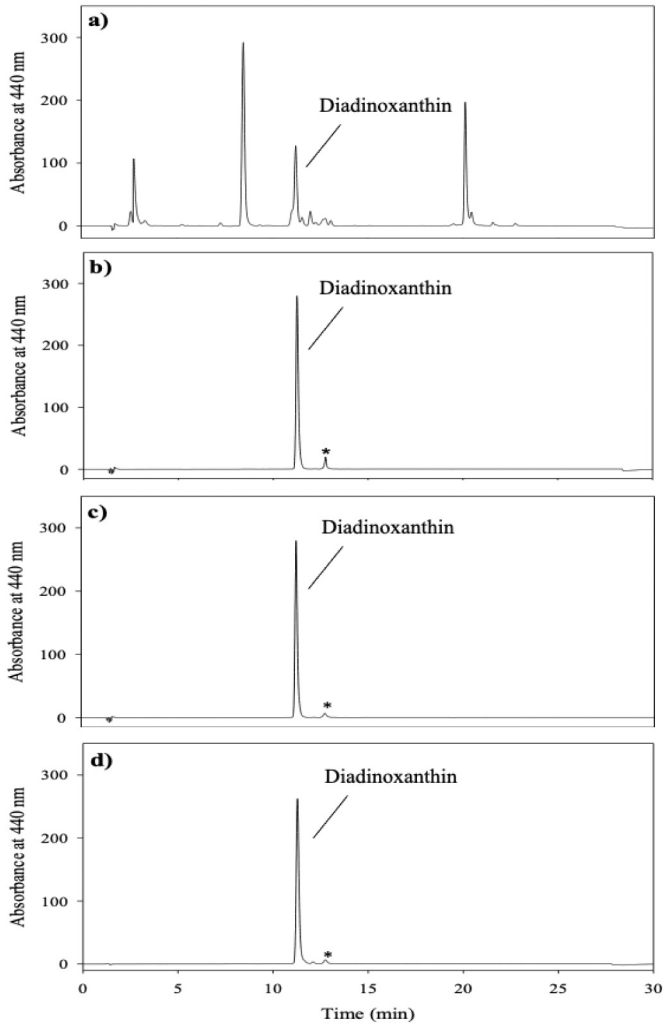

Fig. 6. HPLC–DAD chromatographic profiles of *Phaeodactylum tricornutum* extract (**a**), diadinoxanthin obtained by HPCCC (**b**), diadinonoxanthin purified by gel permeation chromatography (**c**), and commercial diadinoxanthin standard (Sigma-Aldrich) (**d**). Chromatograms were recorded at 440 nm. The peak corresponding to **cis*-diadinoxanthin is indicated.

Table 4
Comparison of upper (UP, stationary) and lower (LP, mobile) phase consumption during HPCCC separation of diadinoxanthin using formulated (F) and non-formulated (NF) liquid phases.

Individual solvent	Two-injections HPCCC				
	NF Total volume (mL)	F			Saved volume (mL)
		UP (mL)	LP (mL)	Total volume (mL)	
n-heptane	329.895	320.265	3.234	323.499	6.396
Ethyl acetate	263.916	96.705	98.742	195.447	68.469
Ethanol	329.895	29.250	197.190	226.440	103.455
Water	197.937	3.780	120.834	124.614	73.323

3.5. Identity confirmation

The identity of the purified pigment was confirmed as diadinoxanthin by combining atmospheric pressure chemical ionization-high-resolution mass spectrometry (APCI-HRMS/MS) with UV–visible spectroscopy, supported by comparison with published reference values [45,54,55] and an authentic commercial standard. Diadinoxanthin is a well-documented xanthophyll carotenoid widely distributed in diatoms, and its complete molecular structure has been established in earlier studies using NMR [21] and complementary spectroscopic techniques. In the present study, structural identity was therefore confirmed by comparison with known analytical characteristics. In the APCI-HRMS/MS spectrum (Fig. 7a), the main molecular ion peak was detected at *m/z* 583.4183 ($[M + H]^+$), consistent with the molecular mass of diadinoxanthin ($C_{40}H_{54}O_3$). Sequential dehydration fragments were observed at *m/z* 565.4056 ($[M + H–H_2O]^+$) and *m/z* 547.3976 ($[M + H–2H_2O]^+$), arising from losses of hydroxyl groups at the terminal ends of the molecule. An additional fragment at *m/z* 491 corresponded to a neutral loss of 92 Da, indicative of toluene (C_7H_8) elimination. These fragmentation patterns matched those previously reported for diadinoxanthin [45,54,55], confirming molecular identity. A MS fragmentation scheme of the target pigment is provided in **Supplementary Material** Fig. S2.

In the HPLC chromatogram of the isolated fraction, a minor secondary peak at a retention time of 12.5 min was also detected (Fig. 6b,c). This peak exhibited an identical MS fragmentation profile to diadinoxanthin (Fig. 7a), indicating that it may represent a geometric isomer rather than a distinct compound. To clarify this, UV–visible spectroscopy was used not for structural elucidation, but specifically to distinguish *cis–trans* isomerism, a well-established application of UV–Vis analysis in carotenoid chemistry. The major purified pigment displayed absorption maxima at 420, 444, and 474 nm (Fig. 7b), characteristic of all-*trans*-diadinoxanthin [54]. In contrast, the minor co-eluting component exhibited absorption peaks at 416, 438, and 466 nm (Fig. 7c), with a pronounced hypsochromic shift and an additional *cis*-band near 336 nm, features diagnostic of a *cis* isomer. Similar spectral shifts have been documented for other carotenoids undergoing photo- or thermally induced *cis-trans* isomerization [44,56]. The occurrence of both isomeric forms likely reflects the inherent instability of carotenoids, whose extended conjugated polyene chains are prone to oxidation and isomerization under light, heat, or chemical stress [1]. Taken together, the concordance of accurate mass measurements, diagnostic MS/MS fragmentation, UV–visible isomeric signatures, chromatographic behavior, and direct comparison with a commercial standard provides unambiguous confirmation that the major pigment isolated by HPCCC is diadinoxanthin, predominantly in its all-*trans* configuration.

Table 5
Projected throughput of the developed HPCCC method to obtain diadinoxanthin from *Phaeodactylum tricornutum* across different HPCCC scales.

Column volume (L)	Throughput (g/h)	Throughput (g/week)	Projected diadinoxanthin yield (g/week)
0.134	0.078*	3.114[a]	0.013
0.980	0.569	22.773[a]	0.099
4.600	2.672	64.136[b]	0.278
8.820	5.124	122.974[b]	0.888
18.000	10.457	250.967[b]	1.088

The throughput values indicate the amount of algae extract processed per hour. [a] Estimates for lab-scale systems are based on 40 h of operation per week. [b] Pilot scale estimates are based on 24 h per week of continuous operation when equipment is available. *Experimental value obtained in this study.

3.6. In vitro assays

3.6.1. Scavenging activity toward DPPH and ABTS

The antiradical capacity of diadinoxanthin was first screened using two complementary radicals, DPPH and ABTS, which assess the hydrogen- and electron-donating properties of antiradical compounds [57]. As shown in Fig. 8a,d, diadinoxanthin exhibited a clear concentration-dependent scavenging activity within the range of 3.125–100 μM. The pigment displayed stronger activity toward ABTS radicals ($EC_{50} = 7.41 \pm 0.11$ μM) than DPPH radicals ($EC_{25} = 12.21 \pm 0.79$ μM), indicating a higher reactivity in hydrophilic radical

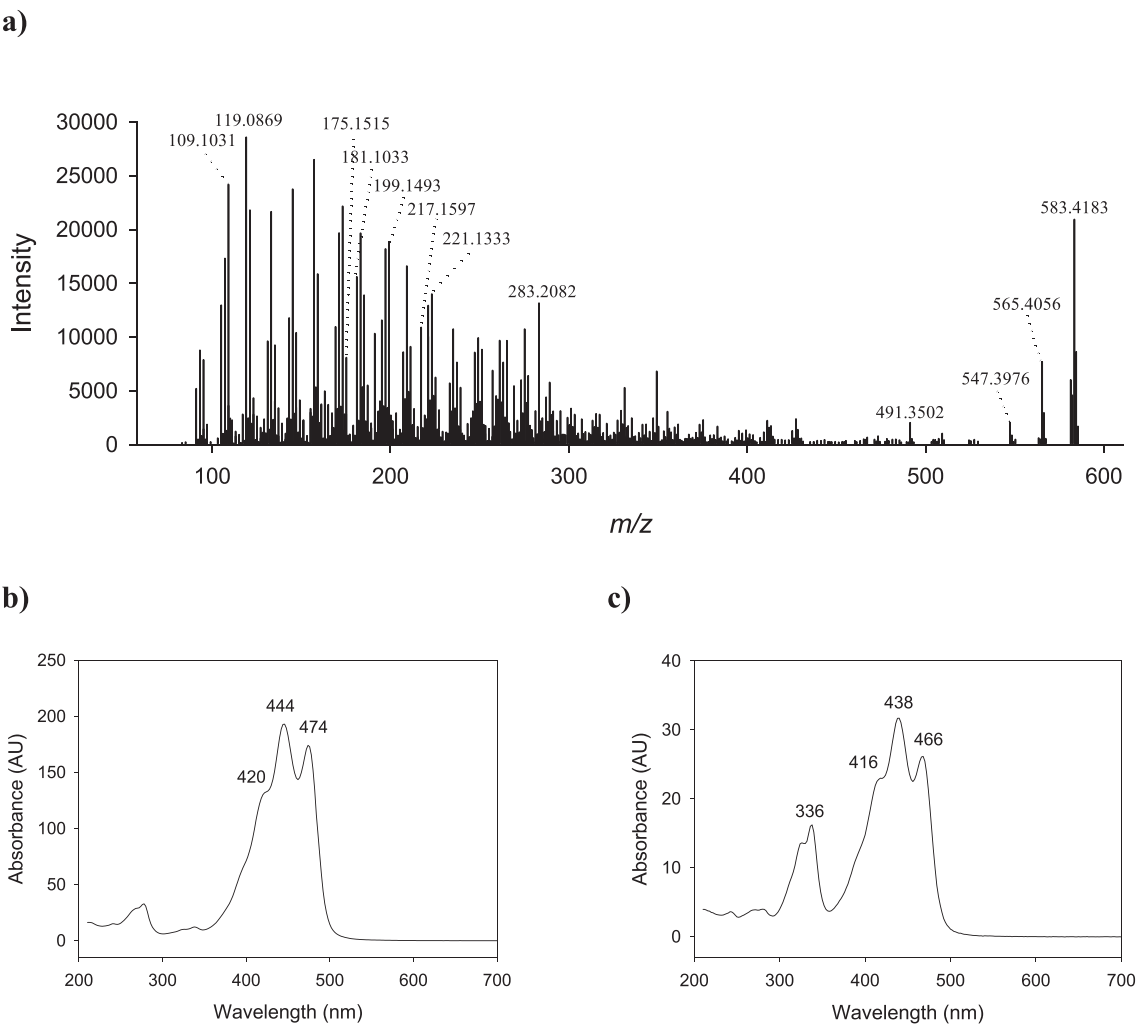

Fig. 7. Atmospheric pressure chemical ionization-high-resolution mass spectrometry (APCI–HRMS) and UV–visible (UV–Vis) spectral characterization of diadinoxanthin isomers obtained by HPCCC. (**a**) APCI-HRMS spectrum of *all-trans*-diadinoxanthin; (**b**) UV–Vis spectrum of all-*trans*-diadinoxanthin; (**c**) UV–Vis spectrum of *cis*-diadinoxanthin.

environments. Quercetin, used as a positive control, showed high scavenging efficiency in both assays, with EC_{50} values of 6.04 ± 0.23 and 5.91 ± 0.19 μM toward DPPH and ABTS, respectively, validating the reliability of the experimental setup. While diadinoxanthin was less potent than quercetin, its activity falls within a biologically relevant range for naturally occurring carotenoids.

For comparison, fucoxanthin, the predominant carotenoid in *P. tricornutum* extracts, was also evaluated (Fig. 8b,e). Diadinoxanthin demonstrated greater scavenging efficiency against both radicals, whereas fucoxanthin showed EC_{50} and EC_{25} values of 10.24 ± 0.14 μM (ABTS) and 22.91 ± 1.35 μM (DPPH), respectively. The superior ABTS scavenging performance of diadinoxanthin may be attributed to its extended conjugated double-bond system and the absence of a carbonyl group, structural features that enhance π-electron delocalization and facilitate stabilization of unpaired electrons, thereby improving radical-scavenging efficiency [21,58]. The free radical scavenging activity of the *P. tricornutum* crude extract was also analyzed for comparative purposes (Fig. 8c,f) and was found to potently scavenge ABTS radicals at concentrations above 125 μg mL^{-1}, in line with the concentration-dependent efficacy of diadinoxanthin and fucoxanthin. The extract was also significantly active against DPPH across the full range of tested concentrations, but only caused a reduction in radical levels greater than 50% at 500 and 1000 μg mL^{-1}. These results confirm that diadinoxanthin possesses antiradical potential, consistent with earlier reports [21], and that its bioactivity was preserved following HPCCC purification. Overall, diadinoxanthin is suggested to be a key contributor to the antiradical capacity of *P. tricornutum* extracts and represents a relevant bioactivity and quality marker for microalgal ingredients.

3.6.2. Nitric oxide and superoxide radical scavenging assay

The significant scavenging effects observed against ABTS and DPPH prompted us to further evaluate and confirm the antiradical activity against physiologically relevant free radicals. Diadinoxanthin showed a weak, non-concentration-dependent effect across 3.125–100 μM, causing reductions in $^{\bullet}NO$ levels ranging from 82.8 to 89.6% (Fig. 8g), while fucoxanthin exhibited no statistically significant effect (Fig. 8h). The estimated EC_{50} value for quercetin (180 ± 15 μM), used here as a positive control, indicates that diadinoxanthin exhibits a considerably weaker scavenging effect. In contrast, the *P. tricornutum* extract displayed a clear concentration-dependent response between 31.25 and 1000 μg mL^{-1}, with statistically significant scavenging effects at concentrations higher than 125 μg mL^{-1} (Fig. 8i), suggesting that $NO^{\bullet}$ scavenging arises from the combined action of multiple antiradical constituents rather than from individual xanthophylls. As shown in Fig. 8j and k, both diadinoxanthin and fucoxanthin exhibit weak scavenging effects toward superoxide ($O_2^{\bullet-}$), in both cases not reducing radical levels by more than 14%, and performing worse than quercetin (EC_{50} = 127 ± 8 μM), once again demonstrating the consistently

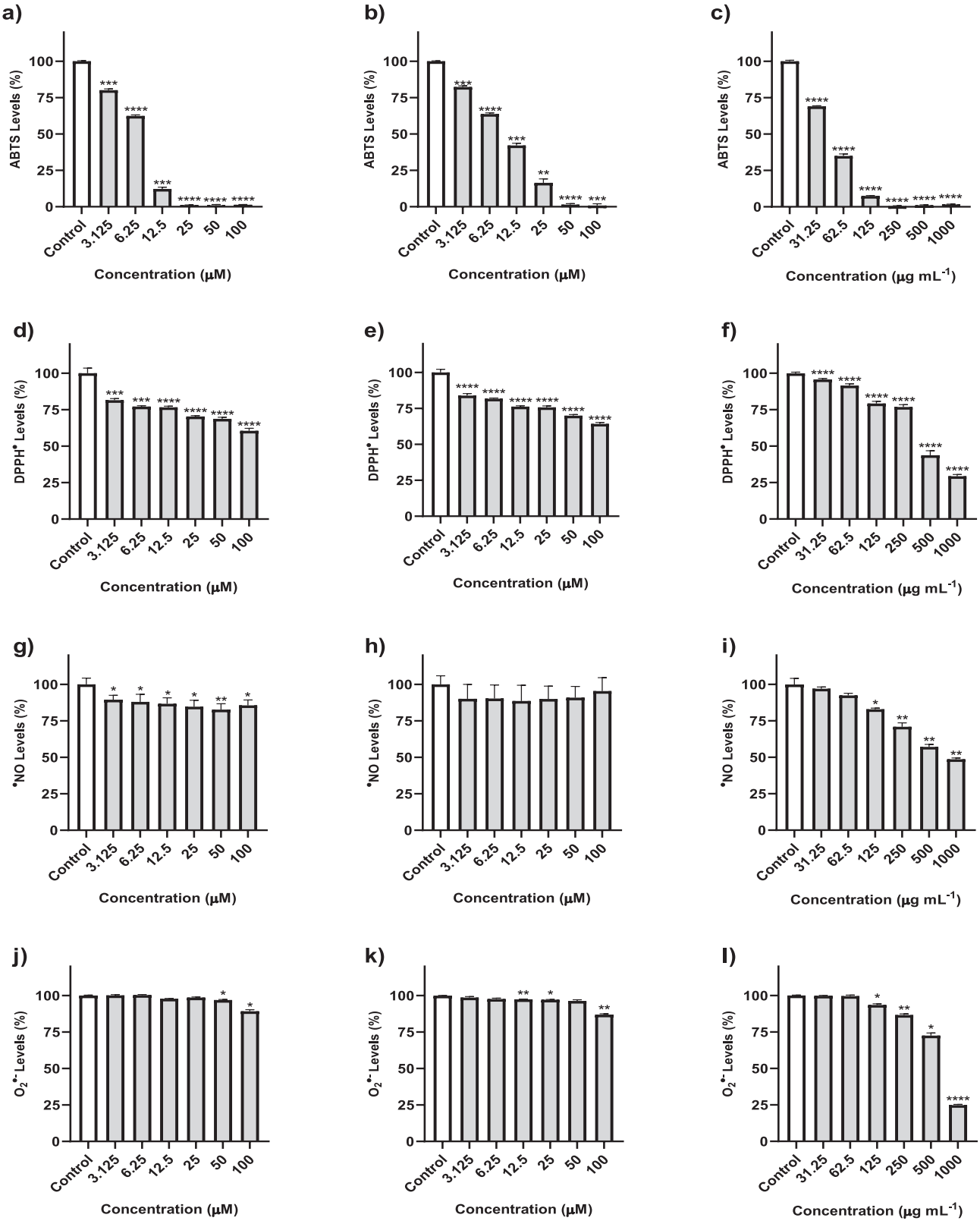

Fig. 8. Free radical scavenging activities of diadinoxanthin (**a**, **d**, **g**, **j**), fucoxanthin (**b**, **e**, **h**, **k**), and *Phaeodactylum tricornutum* extract (**c**, **f**, **i**, **l**) against ABTS (**a**–**c**), DPPH (**d**–**f**), $^{\bullet}$NO (**g**–**i**) and $O_2^{\bullet-}$ (**j**-**l**) radicals. The results are presented as the mean ± SEM values obtained from a minimum of three independent experiments, performed in triplicate. Statistical significance: * $p < 0.05$, ** $p < 0.01$, *** $p < 0.001$, **** $p < 0.0001$.

superior performance of the flavonoid compound. Similar to the results observed for •NO scavenging, the higher antiradical activity of the extract (Fig. 8l) again suggests that other constituents may underlie the observed effects upon $O_2^{\bullet-}$. Biologically, nitric oxide is a signaling molecule that can generate peroxynitrite ($ONOO^-$) through reaction with superoxide, leading to lipid peroxidation, protein nitration, and inflammation. Besides their intrinsic and physiologically controlled production, reactive oxygen species (ROS), namely •NO, $O_2^{\bullet-}$ and $ONOO^-$, can be abnormally induced extrinsically in the skin by UVA, UVB, visible light, infrared radiation, pollutants, and psychological stress, being pivotal contributors to skin aging, skin inflammation or melanoma [59,60]. Thus, efficient •NO scavengers play an essential role in mitigating nitrosative stress [61]. The limited •NO quenching observed for diadinoxanthin suggests its antioxidant activity is mainly oriented toward singlet oxygen and peroxyl radicals, consistent with its photoprotective role in diatoms [1,62]. Opposite trend has been reported for β-carotene [63]. The weak activity of diadinoxanthin in the present assay suggests that, unlike ABTS and DPPH radicals, the conjugated double-bond system plays a minor role in scavenging •NO and superoxide radicals.

3.6.3. Assessment of 5-lipoxygenase enzymatic activity

The enzyme 5-lipoxygenase (5-LOX) plays a central role in the arachidonic acid cascade, catalyzing the formation of leukotrienes and other eicosanoids that mediate inflammatory processes [64]. Alongside the cyclooxygenase (COX) enzymes, 5-LOX constitutes one of the two principal pathways for eicosanoid biosynthesis. While COX-1 and COX-2 are responsible for prostaglandin and thromboxane production, 5-LOX converts arachidonic acid into leukotrienes such as LTB_4, a potent mediator implicated in asthma, atherosclerosis, and cancer. Inhibition of 5-LOX activity is therefore considered a conventional approach for an anti-inflammatory strategy, potentially mitigating the side effects associated with long-term COX inhibition [65]. However, inhibition of 5-LOX also appears to be particularly effective in cutaneous inflammatory diseases, as the enzyme is overexpressed in autoimmune disorders with an inflammatory background, such as systemic sclerosis, and is increasingly recognized as playing a role in the coordination of the tumor inflammatory microenvironment in several cancer types, including melanoma [66,67]. In this study, diadinoxanthin demonstrated a clear, concentration-dependent inhibition of 5-LOX activity across the 25–100 μM range (Fig. 9a) with an IC_{50} value of 40.10 ± 2.32 μM. For comparison, fucoxanthin, the major xanthophyll in *P. tricornutum*, exhibited lower inhibitory activity (IC_{50} = 58.53 ± 6.10 μM) (Fig. 9b). Despite the significant inhibitory effects of both xanthophyll carotenoids, both proved to be less effective than quercetin, herein used as a reference 5-LOX inhibitor (IC_{50} = 7.3 ± 2.0 μM). The crude *P. tricornutum* extract showed significant inhibition at concentrations higher than 125 μg mL^{-1} (Fig. 9c), suggesting that individual carotenoids such as diadinoxanthin contribute substantially to the extract's anti-inflammatory potential.

To the best of our knowledge, this is the first report describing direct inhibition of 5-LOX by diadinoxanthin. Previous studies on fucoxanthin have primarily focused on its ability to downregulate COX-2 expression and suppress prostaglandin E_2 (PGE_2) synthesis, rather than direct enzyme inhibition [68]. Both diadinoxanthin and fucoxanthin contain epoxide functionalities; however, diadinoxanthin is distinguished by the presence of an acetylenic bond (C≡C) within its polyene chain, whereas fucoxanthin is characterized by an allenic bond (C=C=C) and a conjugated keto group within its terminal ring system. These structural differences may influence molecular conformation, electron distribution,

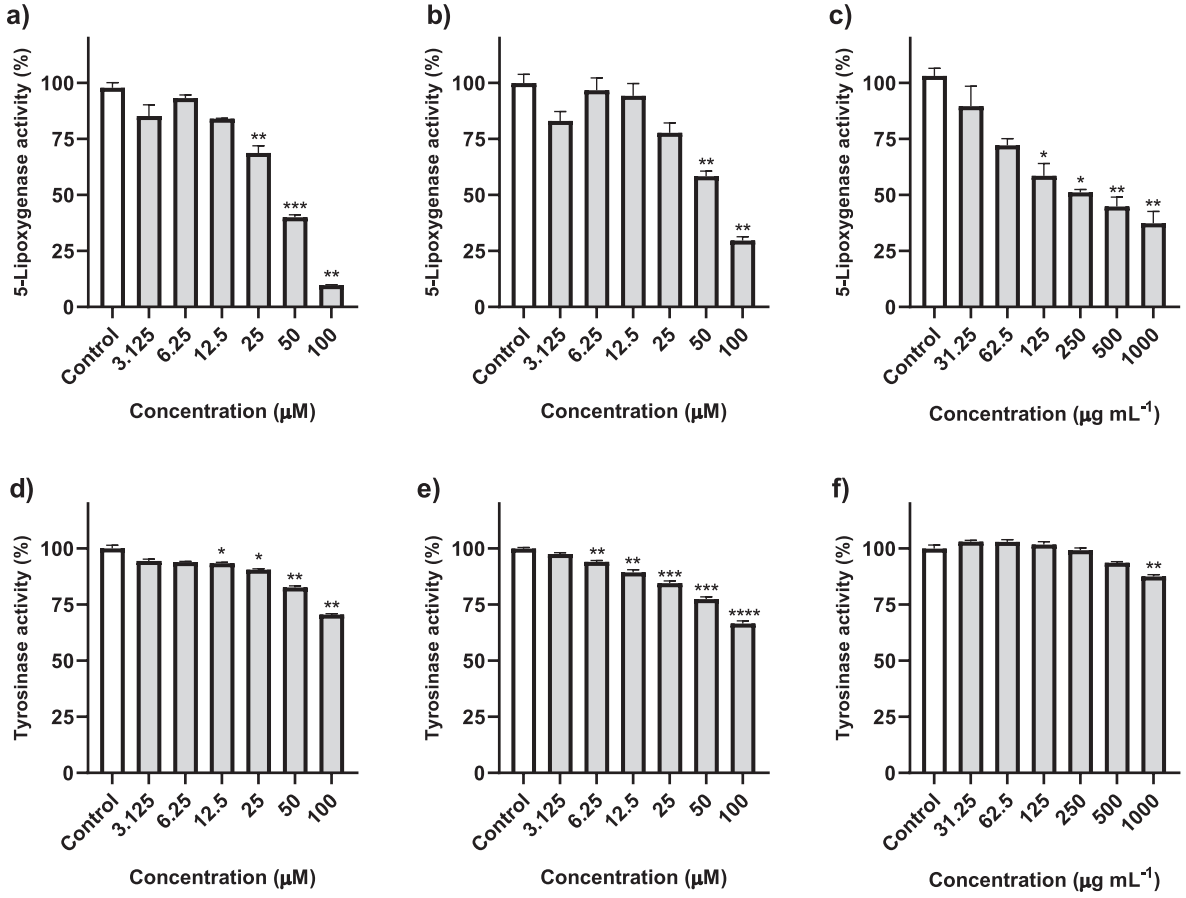

Fig. 9. Effects of diadinoxanthin (**a**, **d**), fucoxanthin (**b**, **e**), and *Phaeodactylum tricornutum* extract (**c**, **f**) on the activity of 5-lipoxygenase (**a-c**) and tyrosinase (**d-f**). Results represent the mean ± SEM of a minimum of three independent experiments, performed in triplicate. *$p < 0.05$, **$p < 0.01$, ***$p < 0.001$, ****$p < 0.0001$.

and interactions within or near the 5-lipoxygenase active site, potentially contributing to differences in inhibitory activity. Epoxy-containing lipids have been reported to interact with LOX enzymes as substrates or metabolizable intermediates [69], suggesting that epoxy-containing carotenoids may interact with LOX catalytic machinery, although not necessarily as true substrates. Importantly, acetylenic moieties are a recognized structural feature of several LOX inhibitors, including acetylenic fatty acids [70], synthetic benzyl propargyl ethers [71], and Atreleuton [72], which can interfere with substrate binding or promote redox-based enzyme inactivation. In this context, the acetylenic bond present in diadinoxanthin may contribute to enhanced interactions with residues involved in substrate positioning or iron-centered catalysis. Conversely, fucoxanthin's allenic bond and polar carbonyl group may influence binding orientation or steric compatibility, potentially resulting in weaker direct inhibition. Nevertheless, definitive structure–activity relationships cannot be established from the present data alone. A comprehensive structure–activity relationship study using additional carotenoid derivatives will be required to fully elucidate the contribution of these functional groups to 5-LOX inhibition. Overall, these findings expand the known biofunctional spectrum of diadinoxanthin and support its consideration as a minor yet biologically relevant anti-inflammatory component of diatom-derived carotenoid mixtures, with potential applicability in cosmetic and dermopharmaceutical formulations targeting inflammatory skin conditions.

3.6.4. Tyrosinase inhibition assay

Tyrosinase is a key copper-containing enzyme responsible for catalyzing melanin biosynthesis, and its overactivity has been predominantly associated with hyperpigmentation disorders such as melasma, age spots, and freckles. However, excessive melanin production underlies a range of dermatological conditions, including melasma, post-inflammatory hyperpigmentation and actinic lentigo, and acts as a key mediator of skin aging [59]. So far, most approved tyrosinase inhibitors have demonstrated clinical utility only as skin-depigmenting agents, mainly due to their weak inhibitory effects, but increasing evidence suggests their potential use as an adjuvant strategy in melanoma therapy [73]. Inhibition of tyrosinase is therefore a central strategy for managing pigmentation-related conditions, with its broader clinical utility being progressively reported, spanning now from cosmetics to drug development [74]. The tyrosinase inhibitory potential of diadinoxanthin was assessed in vitro, revealing weak but concentration-dependent activity over the range of 12.5–100 μM, with an IC_{25} value of 79.18 ± 2.18 μM being estimated (Fig. 9d). For comparative purposes, fucoxanthin and the *P. tricornutum* extract were also tested. Fucoxanthin displayed similarly modest, yet greater, inhibitory effect (IC_{25} = 58.88 ± 8.30 μM) within the 6.25 and 100 μM range (Fig. 9e). As neither diadinoxanthin nor fucoxanthin reached 50% inhibitory capacity toward tyrosinase activity, only IC_{25} values were estimated, but being evident that both compounds displayed lower inhibitory potency than the cosmetic ingredient kojic acid, which showed an estimated IC_{50} of 36.6 ± 0.7 μM as the reference tyrosinase inhibitor. The microalgal extract, tested at 31.25–1000 μg mL^{-1}, showed no detectable tyrosinase inhibition (Fig. 9f), suggesting that individual xanthophyll activity is either masked within the complex pigment matrix or reduced due to interactions that limit bioavailability. Although the observed tyrosinase inhibition is relatively weak, diadinoxanthin could still be valuable in cosmeceutical formulations, particularly when combined with other bioactive compounds. Overall, the combination of even modest enzyme inhibition with established antiradical activity underscores the multifunctional potential of diadinoxanthin, supporting its inclusion in cosmeceutical applications.

3.6.5. Senolytic activity

Senolytic compounds selectively eliminate senescent cells, non-proliferating yet metabolically active cells that accumulate with age and contribute to inflammation, tissue dysfunction, and disease progression [75,76]. The identification of natural senolytics is gaining attention due to their potential applications in anti-aging, nutraceutical, and therapeutic formulations. In the current study, diadinoxanthin exhibited selective, concentration-dependent cytotoxicity (88–264 μM) toward palbociclib-induced senescent human melanoma (SK-MEL-103), while showing minimal effects on proliferating cells (Fig. 10). The *P. tricornutum* extract showed comparable activity, whereas fucoxanthin displayed negligible senolytic effects under the same conditions (data not shown), indicating that diadinoxanthin may be the main contributor to the senolytic potential of the extract. Although diadinoxanthin and fucoxanthin share a carotenoid polyene backbone and both contain epoxide functionalities, only diadinoxanthin exhibited senolytic activity under the conditions tested. This observation suggests that the presence of an epoxide group alone is insufficient to account for senolytic effects. Structural differences between the two carotenoids, including the presence of an acetylenic bond in diadinoxanthin and the more polar conjugated keto functionality in fucoxanthin, may contribute to their distinct biological responses. However, the precise structural features responsible for senolytic activity remain unclear. Further investigation of a broader range of carotenoid derivatives will be required to better elucidate structure–activity relationships in this context. To the best of our knowledge, this study provides the first evidence of senolytic activity associated with diadinoxanthin. These results are particularly relevant in the framework of emerging "one-two punch" cancer therapy strategies, which combine senescence-inducing agents such as palbociclib with senolytic compounds to selectively remove therapy-induced senescent cells and thereby reduce the risk of tumor recurrence [77,78]. Although this work represents an initial screening, the findings

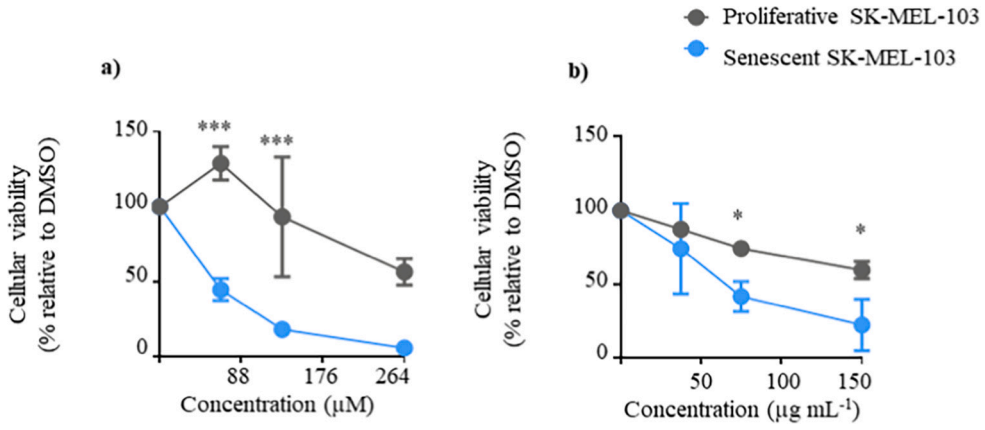

Fig. 10. Senolytic effect of diadinoxanthin (**a**) and *Phaeodactylum tricornutum* extract (**b**) against human melanoma (SK-MEL-103) in proliferation or senescence. The results are presented as the mean ± SEM values obtained from a minimum of three independent experiments. Statistical significance: * $p < 0.05$, *** $p < 0.001$.

highlight diadinoxanthin as a promising lead molecule warranting further investigation to clarify its underlying mechanisms and assess its translational potential in anti-aging and oncology applications.

4. Conclusion

This study demonstrates the feasibility of a scalable HPCCC-based strategy for the targeted recovery of diadinoxanthin from *P. tricornutum*. The developed biphasic solvent system (*n*-heptane/ethyl acetate/ethanol/water, 5:4:5:3, *v/v/v/v*) enabled efficient compound partitioning, achieving high recovery using HPCCC and with reduced solvent consumption. The isolated pigment proved to surpass the well-established bioactive ingredient fucoxanthin in most of the bioactivities assayed, exhibiting superior antiradical, anti-inflammatory, and senolytic properties. Cumulatively, our results support diadinoxanthin as a promising candidate for the development of cosmetic formulations for skin care and anti-aging, as well as a preclinical candidate for drug development in melanoma. Although diadinoxanthin represents a minor carotenoid in diatoms, its strong biofunctional performance supports its inclusion as a quality and bioactivity marker in *P. tricornutum*-derived products. The HPCCC methodology presented here provides a scalable model for developing integrated diatom biorefineries capable of co-producing multiple bioactives. Future work should focus on optimizing culture conditions and applying metabolic engineering strategies to enhance diadinoxanthin yield and process scalability.

CRediT authorship contribution statement

Daniela Bárcenas-Pérez: Writing – review & editing, Writing – original draft, Methodology, Investigation, Formal analysis, Data curation, Conceptualization. **Maria Rita Garcia:** Investigation, Data curation. **Nelson G.M. Gomes:** Writing – review & editing, Investigation, Data curation. **Paula B. Andrade:** Investigation, Data curation. **Arantzazu Sierra-Ramirez:** Investigation, Data curation. **Jakub Zápal:** Investigation, Data curation. **Marek Kuzma:** Investigation, Data curation. **Gergely Ernő Lakatos:** Formal analysis, Data curation. **Martin Lukeš:** Formal analysis, Data curation. **Pavel Hrouzek:** Formal analysis, Data curation. **Pablo J. Fernandez-Marcos:** Investigation, Data curation. **José Cheel:** Writing – review & editing, Writing – original draft, Supervision, Methodology, Investigation, Conceptualization.

Statement of informed consent, human/animal rights

No conflicts, informed consent, human or animal rights applicable.

Funding

This work was supported by the Grant Agency of the University of South Bohemia, Czech Republic (GAJU-04-075/2022/P). Part of this work received financial support from the PT national funds (FCT/MECI, Fundação para a Ciência e Tecnologia and Ministério da Educação, Ciência e Inovação) through the project UID/50006 -Laboratório Associado para a Química Verde - Tecnologias e Processos Limpos.

Declaration of competing interest

The authors declare no conflict of interest.

Acknowledgments

Daniela Bárcenas Pérez gratefully acknowledges the research supervision of Dr. José Cheel (Centre Algatech, Czech Academy of Sciences) during her PhD studies, as well as the University of South Bohemia for providing a PhD scholarship. Maria Rita Garcia thanks FCT for her PhD grant ref. 2024.06435.BD. Nelson G. M. Gomes thanks FCT (Fundação para a Ciência e Tecnologia) for funding through the Scientific Employment Stimulus Individual Call (Ref. 2022.07375.CEECIND); doi:10.54499/2022.07375.CEECIND/CP1724/CT0013.

Appendix A. Supplementary data

Supplementary data to this article can be found online at https://doi.org/10.1016/j.algal.2026.104566.

Data availability

No data was used for the research described in the article.

References

[1] P. Kuczyńska, M. Jemiola-Rzemińska, K. Strzałka, Photosynthetic pigments in diatoms, Mar. Drugs 13 (9) (2015) 5847–5881, https://doi.org/10.3390/md13095847.
[2] L. Pruccoli, M. Balducci, B. Pagliarani, A. Tarozzi, Antioxidant and neuroprotective effects of fucoxanthin and its metabolite fucoxanthinol: a comparative *in vitro* study, Curr. Issues Mol. Biol. 46 (6) (2024) 5984–5998, https://doi.org/10.3390/cimb46060357.
[3] N.M. Sachindra, E. Sato, H. Maeda, M. Hosokawa, Y. Niwano, M. Kohno, K. Miyashita, Radical scavenging and singlet oxygen quenching activity of marine carotenoid fucoxanthin and its metabolites, J. Agric. Food Chem. 55 (21) (2007) 8516–8522, https://doi.org/10.1021/jf071848a.
[4] S. Xia, K. Wang, L. Wan, A. Aifen Li, Q. Hu, C. Zhang, Production, characterization, and antioxidant activity of fucoxanthin from the marine diatom *Odontella aurita*, Mar. Drugs 11 (7) (2013) 2667–2681, https://doi.org/10.3390/md110 72667.
[5] U. Neumann, F. Derwenskus, V.F. Flister, U. Schmid-Staiger, T. Hirth, S.C. Bischoff, Fucoxanthin, a carotenoid derived from *Phaeodactylum tricornutum* exerts antiproliferative and antioxidant activities in vitro, Antioxidants 8 (6) (2019) 183, https://doi.org/10.3390/antiox8060183.
[6] H. Maeda, M. Hosokawa, T. Sashima, K. Funayama, K. Miyashita, Fucoxanthin from edible seaweed, *Undaria pinnatifida*, shows antiobesity effect through UCP1 expression in white adipose tissues, Biochem. Biophys. Res. Commun. 332 (2) (2005) 392–397, https://doi.org/10.1016/j.bbrc.2005.05.002.
[7] N. Oliyaei, M. Moosavi-Nasab, A.M. Tamaddon, N. Tanideh, Antidiabetic effect of fucoxanthin extracted from *Sargassum angustifolium* on streptozotocin-nicotinamide-induced type 2 diabetic mice, Food Sci. Nutr. 9 (7) (2021) 3521–3529, https://doi.org/10.1002/fsn3.2301.
[8] M. Woo, S. Jeon, H. Kim, M. Lee, S. Shin, Y.C. Shin, Y. Park, M. Choi, Fucoxanthin supplementation improves plasma and hepatic lipid metabolism and blood glucose concentration in high-fat fed C57BL/6N mice, Chem. Biol. Interact. 186 (3) (2010) 316–322, https://doi.org/10.1016/j.cbi.2010.05.006.
[9] M.A. Gammone, N. D'Orazio, Anti-obesity activity of the marine carotenoid fucoxanthin, Mar. Drugs 13 (2196) (2015) 2214, https://doi.org/10.3390/md13042196.
[10] K.N. Kim, S.J. Heo, W.J. Yoon, S.M. Kang, G. Ahn, T.H. Yi, Y. Jeon, Fucoxanthin inhibits the inflammatory response by suppressing the activation of NF-κB and MAPKs in lipopolysaccharide-induced RAW264.7 macrophages, Eur. J. Pharmacol. 649 (1–3) (2010) 369–375, https://doi.org/10.1016/j.ejphar.2010.09.032.
[11] S.J. Heo, W.J. Yoon, K.N. Kim, G.N. Ahn, S.M. Kang, D.H. Kang, A. Affan, C. Oh, W. K. Jung, Y.J. Jeon, Evaluation of anti-inflammatory effect of fucoxanthin isolated from brown algae in lipopolysaccharide-stimulated RAW 264.7 macrophages, Food Chem. Toxicol. 48 (2010) 2045–2051, https://doi.org/10.1016/j.fct.2010.05.003.
[12] L.J. Martin, Fucoxanthin and its metabolite fucoxanthinol in cancer prevention and treatment, Mar. Drugs 13 (8) (2015) 4784–4798, https://doi.org/10.3390/md13084784.
[13] D. Pádua, E. Rocha, D. Gargiulo, A.A. Ramos, Bioactive compounds from brown seaweeds: Phloroglucinol, fucoxanthin and fucoidan as promising therapeutic agents against breast cancer, Phytochem. Lett. 14 (2015) 91–98, https://doi.org/10.1016/j.phytol.2015.09.007.
[14] Y. Satomi, Antitumor and cancer-preventative function of fucoxanthin: A marine carotenoid, Anticancer Res. 37 (4) (2017) 1557–1562, https://doi.org/10.21873/anticanres.11484.
[15] L. Hu, W. Chen, F. Tian, C. Yuan, H. Wang, H. Yue, Neuroprotective role of fucoxanthin against cerebral ischemic/reperfusion injury through activation of Nrf2/HO-1 signaling, Biomed. Pharmacother. 106 (1) (2018) 1484–1489, https://doi.org/10.1016/j.biopha.2018.07.088.
[16] Algatech. FucoVital™. https://www.algatech.com/algatech-product/fucovital, (Accesed 12 August, 2025).
[17] Alga-Health. NutriXanthin™ and DermaXanthin™. https://alga-health.com/products, (Accesed 12 August, 2025).
[18] Microphyt. Gamephyt™ and BrainPhyt™. https://microphyt.eu/, (Accesed 12 August, 2025).
[19] G. Chini Zittelli, R. Lauceri, C. Faraloni, A.M. Silva Benavides, G. Torzillo, Valuable pigments from microalgae: Phycobiliproteins, primary carotenoids, and fucoxanthin, Photochem. Photobiol. Sci. 22 (3) (2023) 1733–1789, https://doi.org/10.1007/s43630-023-00407-3.

[20] W. Tokarek, S. Listwan, J. Pagacz, P. Leśniak, D. Latowski, Column chromatography as a useful step in purification of diatom pigments, Acta Biochim. Pol. 63 (3) (2016) 443–447, https://doi.org/10.18388/abp.2016_1369.
[21] G. Zhuang, Y. Ye, J. Zhao, C. Zhou, J. Zhu, Y. Li, J. Zhang, X. Yan, Valorization of *Phaeodactylum tricornutum* for integrated preparation of diadinoxanthin and fucoxanthin, Bioresour. Technol. 385 (2023) 129412, https://doi.org/10.1016/j.biortech.2023.129412.
[22] P. Kuczyńska, M. Jemiola-Rzemińska, Isolation and purification of all-trans diadinoxanthin and all-trans diatoxanthin from the diatom *Phaeodactylum tricornutum*, J. Appl. Phycol. 29 (1) (2017) 79–87, https://doi.org/10.1007/s10811-016-0961-x.
[23] Y. Ito, Golden rules and pitfalls in selecting optimum conditions for high-speed counter-current chromatography, J. Chromatogr. A 1065 (2) (2005) 145–168, https://doi.org/10.1016/j.chroma.2004.12.044.
[24] A. Berthod, T. Maryutina, B. Spivakov, O. Shpigun, I. Sutherland, Countercurrent chromatography in analytical chemistry (IUPAC Technical Report), Pure Appl. Chem. 81 (2) (2009) 355–387, https://doi.org/10.1351/PAC-REP-08-06-05.
[25] I.A. Sutherland, Recent progress on the industrial scale-up of counter-current chromatography, J. Chromatogr. A 1151 (1–2) (2007) 6–13, https://doi.org/10.1016/j.chroma.2007.01.143.
[26] X. Xiao, X. Si, Z. Yuan, X. Xu, G. Li, Isolation of fucoxanthin from edible brown algae by microwave-assisted extraction coupled with high-speed countercurrent chromatography, J. Sep. Sci. 35 (17) (2012) 2313–2317, https://doi.org/10.1002/jssc.201200231.
[27] S.M. Kim, Y.F. Shang, B.H. Um, A preparative method for isolation of fucoxanthin from *Eisenia bicyclis* by centrifugal partition chromatography, Phytochemical analysis: PCA 22 (4) (2011) 322–329, https://doi.org/10.1002/pca.1283.
[28] R. Gonçalves de Oliveira-Júnior, R. Grougnet, P. Bodet, A. Bonnet, E. Nicolau, A. Jebali, J. Rumin, L. Picot, Updated pigment composition of *Tisochrysis lutea* and purification of fucoxanthin using centrifugal partition chromatography coupled to flash chromatography for the chemosensitization of melanoma cells, Algal Res. 51 (2020) 102035, https://doi.org/10.1016/j.algal.2020.102035.
[29] D. Bárcenas-Pérez, A. Střížek, P. Hrouzek, J. Kopecký, M. Barradas, A. Sierra-Ramirez, P.J. Fernandez-Marcos, J. Cheel, Production of fucoxanthin from *Phaeodactylum tricornutum* using high performance countercurrent chromatography retaining its FOXO3 nuclear translocation-inducing effect, Mar. Drugs 19 (9) (2021) 517, https://doi.org/10.3390/md19090517.
[30] D. Bárcenas-Pérez, D. Gomes, C. Parreira, L. Costa, J. Cheel, Recovery of β-carotene from microalga *Dunaliella* sp. by HPCCC, Processes 13 (6) (2025) 1812, https://doi.org/10.3390/pr13061812.
[31] Y. Yang, S. Guo, D. Gu, A strategy to process hundred-gram level complex sample using liquid-liquid-refining extraction and consecutive counter-current chromatography: *Toona sinensis* case study, J. Chromatogr. A 1661 (2022) 462717, https://doi.org/10.1016/j.chroma.2021.462717.
[32] Y. Yang, Y. Wang, W. Zeng, J. Tian, X. Zhao, J. Han, D. Huang, D. Gu, A strategy based on liquid-liquid-refining extraction and high-speed counter-current chromatography for the bioassay-guided separation of active compounds from *Taraxacum mongolicum*, J. Chromatogr. A 1614 (2020) 460727, https://doi.org/10.1016/j.chroma.2019.460727.
[33] R.C. Starr, J.A. Zeikus, UTEX–the culture collection of algae at the university of Texas at Austin 1993 list of cultures, J. Phycol. 29 (1993) 106, https://doi.org/10.1111/j.0022-3646.1993.00106.x.
[34] J. Cheel, M. Minceva, P. Urajová, R. Aslam, P. Hrouzek, J. Kopecký, Separation of aeruginosin-865 from cultivated soil cyanobacterium (*Nostoc* sp.) by centrifugal partition chromatography combined with gel permeation chromatography, Nat. Prod. Commun. 10 (10) (2015) 1719–1722, https://doi.org/10.1177/1934578X15010010.
[35] J. Cheel, P. Urajová, J. Hájek, P. Hrouzek, M. Kuzma, E. Bouju, K. Faure, J. Kopecký, Separation of cyclic lipopeptide puwainaphycins from cyanobacteria by countercurrent chromatography combined with polymeric resins and HPLC, Anal. Bioanal. Chem. 409 (4) (2017) 917–930, https://doi.org/10.1007/s00216-016-0066-z.
[36] Y. Ito, W.D. Conway, Experimental observations of the hydrodynamic behavior of solvent systems in high-speed counter-current chromatography. III. Effects of physical properties of the solvent systems and operating temperature on the distribution of two-phase solvent systems, J. Chromatogr. 301 (2) (1984) 405–414, https://doi.org/10.1016/s0021-9673(01)89214-1.
[37] I.A. Sutherland, Liquid stationary phase retention and resolution in hydrodynamic CCC, Compr. Anal. Chem. 38 (2002) 159–176, https://doi.org/10.1016/S0166-526X(02)80009-5.
[38] J. Kang, D. Gu, T. Wu, M. Wang, H. Zhang, H. Guo, Y. Yin, Y. Yang, J. Tian, An approach based upon the consecutive separation and the economical two-phase solvent system preparation using UNIFAC mathematical model for increasing the yield of high-speed counter-current chromatography, Sep. Purif. Technol. 162 (2016) 142–147, https://doi.org/10.1016/j.seppur.2016.02.026.
[39] G. Schmeda-Hirschmann, J.A. Rodriguez, C. Theoduloz, S.L. Astudillo, G. E. Feresin, A. Tapia, Free-radical scavengers and antioxidants from *Peumus boldus* Mol. ("Boldo"), Free Radic. Res. 37 (4) (2003) 447–452, https://doi.org/10.1080/1071576031000090000.
[40] H. Osman, A.A. Rahim, N.M. Isa, N.M. Bakhir, Antioxidant activity and phenolic content of *Paederia foetida* and *Syzygium aqueum*, Molecules (Basel, Switzerland) 14 (3) (2009) 970–978, https://doi.org/10.3390/molecules14030970.
[41] M.R. Garcia, F. Ferreres, T. Mineiro, R.A. Videira, Á. Gil-Izquierdo, P.B. Andrade, V. Seabra, D. Dias-da-Silva, N.G. Gomes, Mexican calea (*Calea zacatechichi* Schltdl.) interferes with cholinergic and dopaminergic pathways and causes neuroglial toxicity, J. Ethnopharmacol. 337 (2025) 118915, https://doi.org/10.1016/j.jep.2024.118915.
[42] P. Cebollada, N.G. Gomes, P.B. Andrade, V. López, An integrated *in vitro* approach on the enzymatic and antioxidant mechanisms of four commercially available essential oils (*Copaifera officinalis, Gaultheria fragrantissima, Helichrysum italicum,* and *Syzygium aromaticum*) traditionally used topically for their anti-inflammatory effects, Front. Pharmacol. 14 (2024) 1310439, https://doi.org/10.3389/fphar.2023.1310439.
[43] F. Triana-Martínez, P. Picallos-Rabina, S. Da Silva-Álvarez, F. Pietrocola, S. Llanos, V. Rodilla, E. Soprano, P. Pedrosa, A. Ferreirós, M. Barradas, F. Hernández-González, M. Lalinde, N. Prats, C. Bernadó, P. González, M. Gómez, M. P. Ikonomopoulou, P.J. Fernández-Marcos, T. García-Caballero, P. Del Pino, M. Collado, Identification and characterization of Cardiac Glycosides as senolytic compounds, Nat. Commun. 10 (1) (2019) 4731, https://doi.org/10.1038/s41467-019-12888-x.
[44] T. Fábryová, J. Cheel, D. Kubáč, P. Hrouzek, D.L. Vu, L. Tůmová, J. Kopecký, Purification of lutein from the green microalgae *Chlorella vulgaris* by integrated use of a new extraction protocol and a multi-injection high performance counter-current chromatography (HPCCC), Algal Res. 41 (2019) 101574, https://doi.org/10.1016/j.algal.2019.101574.
[45] G.E. Lakatos, K. Štěrbová, D. Bárcenas-Pérez, T. Grivalský, J. Câmara Manoel, M. Mylenko, J. Cheel, J. Nyári, R. Wirth, K.L. Kováacs, J. Kopecký, J. Elster, J. Masojídek, *Tribonema* cf. *minus* cultivation in thin-layer raceway pond to uncover its biotechnological potential, J. Appl. Phycol. 37 (2025) 2231–2244, https://doi.org/10.1007/s10811-025-03554-5.
[46] J. Renault, J. Nuzillard, O. Intes, A. Maciuk, Solvent systems, Compr. Anal. Chem. 38 (2002) 49–83, https://doi.org/10.1016/S0166-526X(02)80006-X.
[47] European Parliament and Council, Directive 2009/32/EC of the European Parliament and of the Council of 23 April 2009 on the approximation of the laws of the Member States on extraction solvents used in the production of foodstuffs and food ingredients (Recast), Off. J. Eur. Union L 140 (2023) 3–11. https://eur-lex.europa.eu/legal-content/EN/TXT/?uri=CELEX%3A32009L0032. (Accessed 1 October 2025).
[48] F.G. Calvo-Flores, M.J. Monteagudo-Arrebola, J.A. Dobado, J. Isac-García, Green and bio-based solvents, Topics in current chemistry (Cham) 376 (3) (2018) 18, https://doi.org/10.1007/s41061-018-0191-6.
[49] European Medicines Agency, ICH Q3C (R9) guideline: Impurities — guideline for residual solvents (Step 5), 2024. https://www.ema.europa.eu/en/documents/scientific-guideline/ich-q3c-r9-guideline-impurities-guideline-residual-solvents-step-5_en.pdf. (Accessed 1 October 2025).
[50] U.S. Food and Drug Administration, Q3C — Tables and list: Guidance for industry (Revision 4), 2018. https://www.fda.gov/media/133650/download. (Accessed 1 October 2025).
[51] European Parliament and Council, Regulation (EC) No. 1223/2009 on cosmetic products (recast), Off. J. Eur. Union L 342 (2025) 59. https://eur-lex.europa.eu/legal-content/EN/TXT/?uri=CELEX%3A02009R1223-20250901. (Accessed 1 October 2025).
[52] P. Wood, S. Ignatova, L. Janaway, D. Keay, D. Hawes, I. Garrard, I.A. Sutherland, Counter-current chromatography separation scaled up from an analytical column to a production column, J. Chromatogr. A 1151 (1–2) (2007) 25–30, https://doi.org/10.1016/j.chroma.2007.02.014.
[53] S. Li, S. He, S. Zhong, X. Duan, H. Ye, J. Shi, A. Peng, L. Chen, Elution–extrusion counter-current chromatography separation of five bioactive compounds from Dendrobium chrysototxum Lindl, J. Chromatogr. A 1218 (20) (2011) 3124–3128, https://doi.org/10.1016/j.chroma.2011.03.015.
[54] R. Frassanito, M. Cantonati, M. Tardìo, I. Mancini, G. Guella, On-line identification of secondary metabolites in freshwater microalgae and cyanobacteria by combined liquid chromatography-photodiode array detection-mass spectrometric techniques, J. Chromatogr. A 1082 (1) (2005) 33–42, https://doi.org/10.1016/j.chroma.2005.02.066.
[55] B. Guo, B. Liu, B. Yang, P. Sun, X. Lu, J. Liu, F. Chen, Screening of Diatom strains and characterization of *Cyclotella cryptica* as a potential fucoxanthin producer, Mar. Drugs 14 (7) (2016) 125, https://doi.org/10.3390/md14070125.
[56] M. Nováková, T. Fábryová, D. Vokurková, I. Doležková, J. Kopecký, P. Hrouzek, L. Tůmová, J. Cheel, Separation of the glycosylated carotenoid myxoxanthophyll from Synechocystis salina by HPCCC and evaluation of its antioxidant, tyrosinase inhibitory and immune-stimulating properties, Separations 7 (4) (2020) 73, https://doi.org/10.3390/separations7040073.
[57] K. Schaich, X. Tian, J. Xie, Hurdles and pitfalls in measuring antioxidant efficacy: A critical evaluation of ABTS, DPPH, and ORAC assays, J. Funct. Foods 14 (2015) 111–125, https://doi.org/10.1016/j.jff.2015.01.043.
[58] N. Coulombier, T. Jauffrais, N. Lebouvier, Antioxidant compounds from microalgae: a review, Mar. Drugs 19 (10) (2021) 549, https://doi.org/10.3390/md19100549.
[59] J. Chen, Y. Liu, Z. Zhao, J. Qiu, Oxidative stress in the skin: Impact and related protection, Int. J. Cosmet. Sci. 43 (5) (2021) 495–509, https://doi.org/10.1111/ics.12728.
[60] K. Yarlagadda, J. Hassani, I.P. Foote, J. Markowitz, The role of nitric oxide in melanoma, Biochim. Biophys. Acta Rev. Cancer 1868 (2) (2017) 500–509, https://doi.org/10.1016/j.bbcan.2017.09.005.
[61] A.J.P.O. de Almeida, J.C.P.L. de Oliveira, L.V. da Silva Pontes, J.F. de Souza Júnior, T.A.F. Gonçalves, S.H. Dantas, M.S. de Almeida Feitosa, A.O. Silva, I.A. de Medeiros, ROS: basic concepts, sources, cellular signaling, and its implications in aging pathways, Oxidative Med. Cell. Longev. (2022) 1225578, https://doi.org/10.1155/2022/1225578.

[62] J. Lavaud, B. Rousseau, H.J. van Gorkom, A.L. Etienne, Influence of the diadinoxanthin pool size on photoprotection in the marine planktonic diatom *Phaeodactylum tricornutum*, Plant Physiol. 129 (3) (2002) 1398–1406, https://doi.org/10.1104/pp.002014.
[63] R.M. Han, H. Cheng, R. Feng, D.D. Li, W. Lai, J.P. Zhang, L.H. Skibsted, β-Carotene As a Lipophilic Scavenger of Nitric Oxide, J. Phys. Chem. B 118 (40) (2014) 11659–11666, https://doi.org/10.1021/jp5075626.
[64] S. Sinha, M. Doble, S.L. Manju, 5-Lipoxygenase as a drug target: A review on trends in inhibitors structural design, SAR and mechanism based approach, Bioorg. Med. Chem. 27 (17) (2019) 3745–3759, https://doi.org/10.1016/j.bmc.2019.06.040.
[65] M. Rudrapal, W.A. Eltayeb, G. Rakshit, A.A. El-Arabey, J. Khan, S.M. Aldosari, B. Alshehri, M. Abdalla, Dual synergistic inhibition of COX and LOX by potential chemicals from Indian daily spices investigated through detailed computational studies, Sci. Rep. 13 (1) (2023) 8656, https://doi.org/10.1038/s41598-023-35161-0.
[66] M. Romano, J. Claria, Cyclooxygenase-2 and 5-lipoxygenase converging functions on cell proliferation and tumor angiogenesis: implications for cancer therapy, FASEB journal: official publication of the Federation of American Societies for Experimental Biology 17 (14) (2003) 1986–1995, https://doi.org/10.1096/fj.03-0053rev.
[67] O. Kowal-Bielecka, O. Distler, M. Neidhart, P. Künzler, J. Rethage, M. Nawrath, A. Carossino, T. Pap, U. Müller-Ladner, B.A. Michel, Evidence of 5-lipoxygenase overexpression in the skin of patients with systemic sclerosis: A newly identified pathway to skin inflammation in systemic sclerosis, Arthritis Rheum. 44 (8) (2001) 1865–1875, https://doi.org/10.1002/1529-0131(200108)44:8<1865::AID-ART325>3.0.CO;2-M.
[68] H. Xiao, J. Zhao, C. Fang, Q. Cao, M. Xing, X. Li, J. Hou, A. Ji, S. Song, Advances in studies on the pharmacological activities of fucoxanthin, Mar. Drugs 18 (12) (2020) 634, https://doi.org/10.3390/md18120634.
[69] T. Teder, W.E. Boeglin, A.R. Brash, Lipoxygenase-catalyzed transformation of epoxy fatty acids to hydroxy-endoperoxides: A potential P450 and lipoxygenase interaction, J. Lipid Res. 55 (12) (2014) 2587–2596, https://doi.org/10.1194/jlr.M054072.
[70] H. Kühn, K. Hayess, H.G. Holzhütter, D.A. Zabolotzski, G.I. Myagkova, T. Schewe, Inactivation of 15-lipoxygenases by acetylenic fatty acids, Biomed. Biochim. Acta 50 (7) (1991) 835–839.
[71] N.B. Barhate, M.C. Reddy, P.S. Reddy, R.D. Wakharkar, P. Reddanna, Synthesis and biochemical evaluation of benzyl propargyl ethers as inhibitors of 5-lipoxygenase, Indian J. Biochem. Biophys. 39 (4) (2002) 264–273.
[72] S. Sinha, M. Doble, S.L. Manju, 5-Lipoxygenase as a drug target: A review on trends in inhibitors structural design, SAR and mechanism based approach, Bioorg. Med. Chem. 27 (17) (2019) 3745–3759, https://doi.org/10.1016/j.bmc.2019.06.040.
[73] Y. Li, K. Yang, L. Zhao, Tyrosinase inhibitors as melanoma sensitizers: Boosting therapeutic efficacy, Superlattice. Microst. 200 (2025) 100109, https://doi.org/10.1016/j.supmat.2025.100109.
[74] A. Doğan, S. Akocak, Natural products as tyrosinase inhibitors, The Enzymes 56 (2024) 85–109, https://doi.org/10.1016/bs.enz.2024.06.002.
[75] J.L. Kirkland, T. Tchkonia, Senolytic drugs: From discovery to translation, J. Intern. Med. 288 (5) (2020) 518–536, https://doi.org/10.1111/joim.13141.
[76] E.O. Wissler Gerdes, Y. Zhu, T. Tchkonia, J.L. Kirkland, Discovery, development, and future application of senolytics: Theories and predictions, FEBS J. 287 (12) (2020) 2418–2427, https://doi.org/10.1111/febs.15264.
[77] T. Jost, L. Heinzerling, R. Fietkau, M. Hecht, L.V. Distel, Palbociclib induces senescence in melanoma and breast cancer cells and leads to additive growth arrest in combination with irradiation, Front. Oncol. 11 (2021) 740002, https://doi.org/10.3389/fonc.2021.740002.
[78] I. Galiana, B. Lozano-Torres, M. Sancho, M. Alfonso, A. Bernardos, V. Bisbal, M. Serrano, R. Martínez-Máñez, M. Orzáez, Preclinical antitumor efficacy of senescence-inducing chemotherapy combined with a nanoSenolytic, J. Control. Release 323 (2020) 624–634, https://doi.org/10.1016/j.jconrel.2020.04.045.